Microfluid Nanofluid (2008) 4:53–79
DOI 10.1007/s10404-007-0223-y

REVIEW

Optofluidic integration for microanalysis

Hamish C. Hunt · James S. Wilkinson

Received: 1 March 2007 / Accepted: 25 July 2007 / Published online: 11 September 2007

Abstract This review describes recent research in the application of optical techniques to microfluidic systems for chemical and biochemical analysis. The "lab-on-a-chip" presents great benefits in terms of reagent and sample consumption, speed, precision, and automation of analysis, and thus cost and ease of use, resulting in rapidly escalating adoption of microfluidic approaches. The use of light for detection of particles and chemical species within these systems is widespread because of the sensitivity and specificity which can be achieved, and optical trapping, manipulation and sorting of particles show significant benefits in terms of discrimination and reconfigurability. Nonetheless, the full integration of optical functions within microfluidic chips is in its infancy, and this review aims to highlight approaches, which may contribute to further miniaturisation and integration.

Keywords Lab-on-a-chip · Microfluidics · Optical detection · Optical trapping · Integrated optics · Optofluidics

1 Introduction

The convergence of microfabrication technologies, novel materials systems, and techniques for chemical and biochemical analysis is enabling the realisation of the lab-on-a-chip (LoC) or micro-total analysis system (μTAS) (Manz et al. 1990). This research is driven by the demand for fast, low-cost, automated chemical analysis using minimal sample and reagent volumes, in a multiplicity of applications (deMello 2006), including interrogation of individual molecules (Craighead 2006). The scale of integration, low cost and robustness of microfabrication approaches enabled the ubiquitous presence of the mobile phone, hand-held computer and CCD camera, to name a few, in the last century. It is often suggested that products incorporating LoC technology will find similarly widespread use early in this century, for example in personal medicine, food safety, water management and security. Cost and reliability for use by non-specialist personnel will be key issues in achieving this goal, which could advance personalised preventative medicine and public safety, and improve efficiency in food and water use.

As its name suggests, the LoC requires integration of many of the tools found in the (bio)chemistry laboratory. These may include means for sample and reagent presentation such as channels, pumps and valves, chambers for mixing and reaction, heaters for reaction control, devices for trapping, separation and selection, devices for cell lysis, and for chemical analysis (El-Ali et al. 2006). The last decade has seen rapid growth in demonstrations of these functions in chips fabricated using either "hard lithography" in semiconductors or glass or "soft lithography" (Xia and Whitesides 1998) in polymers such as PDMS. The former builds upon the functionality of silicon MEMS and the enormous infrastructure of the microelectronics industry and points to its example of cost reduction in complex electronic systems. The latter exploits the benefits of improved compatibility with biological systems and the simplicity of rapid prototyping in polymers. The emergence of preferred materials for the LoC will depend upon the degree to which components can be standardised and selected for integration to satisfy large-volume applications.

H. C. Hunt · J. S. Wilkinson (✉)
Optoelectronics Research Centre, University of Southampton, Highfield, Southampton, Hampshire SO17 1BJ, UK
e-mail: jsw@orc.soton.ac.uk

Optical approaches are the most widely used for chemical analysis in microsystems, as they have an excellent track-record in chemical analysis, usually show the lowest limits of detection (Lechuga 2007) and provide the greatest chemical or morphological information on the species being analysed. More recently there has been increasing interest in using optical forces as a non-contact means for trapping and separation in microsystems, and for driving pumps. The use of light for "optoporation" of cells in microsystems has also been demonstrated (Soughayer et al. 2000). Users of microfluidic systems for (bio)chemical analysis are familiar with conventional optical systems for chemical analysis and increasingly with the optical manipulation approaches first demonstrated by Ashkin (1970). However, the majority of optical functions demonstrated in microfluidic systems use external micro-optical systems, or hybrid embedding of optical fibres, which, while providing much flexibility, do not offer the robustness, stability, operator-independence, and potential for mass manufacture of fully integrated approaches.

Integrated optics, first proposed by Miller (1969), allows the construction of optical circuits in or on planar substrates, guiding and processing light in dielectric cores of elevated refractive index defined using photolithography. The original motivation for this innovation was in optical telecommunications, but its application to chemical sensing was soon demonstrated in 1974 (Mitchell 1977), where bilirubin in neonatal whole blood was measured in a waveguide evanescent field. Integrated optics is widely used in biosensing and chemical sensing research, but there have been rather few demonstrations in true microfluidic systems. Until recently, most integrated optical circuits consisted of only one or two devices, but the field appears to be maturing with a drive for standardisation of materials, devices and interfaces, allowing much denser integration (Smit et al. 2007), and proposals for photonic circuit foundries which will allow "fab-less" researchers with design and measurement tools to access high-quality device fabrication. The confluence of integrated optics with integrated fluidics in the future LoC shows great potential.

Many excellent reviews of microfluidics (Erickson and Li 2004) for cell manipulation and analysis (Yi et al. 2006a), μTAS (Dittrich et al. 2006), optical manipulation (Dholakia and Reece 2006), and optofluidic devices for non-chemical applications (Psaltis et al. 2006), have recently been published, and this paper does not set out to revisit these topics comprehensively. Instead, the present review focuses on recent advances in the field of full optofluidic integration for (bio)chemical analysis in microsystems, where optical functions have been incorporated in a microfluidic system, and especially where the demonstration of an optical function appears to lend itself to an integrated approach.

2 Optical trapping and separation

A key LoC function is the isolation and trapping of individual entities such as biological cells to allow detailed analysis, and separation of cell types among large populations according to size, for example, before analysis. The most common approaches employ hydrodynamic trapping (Khademhosseini et al. 2005), switched electro-osmotic flow (Fu et al. 1999) or dielectrophoresis (Holmes et al. 2006), but configurations, which employ light have advantages in terms of increased flexibility of liquid medium composition (Wang et al. 2005) and excellent discrimination (Hart et al. 2006). The principles and state-of-the art of optical manipulation are extensively reviewed in (Dholakia and Reece 2006). In short, the forces at work may be broadly described as the "radiation pressure" (RP) forces driving particles in the direction of light propagation and the gradient forces, similar to those exploited in dielectrophoresis (DEP), driving particles of higher refractive index than the surrounding medium to the region of maximum optical intensity. Thus in a weakly focussed (or weakly diffracting) beam, a particle is drawn onto the beam axis and propelled along it, while in a tightly focussed beam or optical tweezer (Ashkin et al. 1986), the forward-directed RP forces may be balanced by the backward-directed gradient forces to trap the particle near the focus, as rapid diffraction leads to a large intensity gradient towards the focus. While optical forces have been used to trap and cool atoms in vacuum, particles of diameters from a few tens of nanometres to ten microns or so can be stably trapped in liquid samples using typical optical components. In this section the use of freely propagating light, evanescent fields and photonic landscapes in microfluidic devices are reviewed, with emphasis on the potential for integration of the optical functions.

2.1 Unguided optical trapping and separation

Optical manipulation using externally focussed beams in microfluidic systems sheds light on the potential applications, advantages and disadvantages of integrated approaches. The use of longitudinal optical propulsion for Chinese hamster ovary cell sorting using radiation pressure was demonstrated by Buican et al (1987) as the "basis of a miniaturized and automated cell biology laboratory". Terray et al. (2005) exploited optical propulsion in a weakly focussed beam combined with opposing fluid flow in a microfluidic system to achieve optical separation or chromatography (Imasaka 1998) of *Bacillus anthracis* spores and mulberry pollen, dependent upon particle size and refractive index. This was followed, using the configuration shown in Fig. 1, by separation of *B. anthracis* and

B. thuringiensis (Hart et al. 2006) and sample concentration in which every cell of the selected type flowing in the channel was sorted (Hart et al. 2007). Another approach to microfluidic optophoresis was demonstrated by Zhang et al. (2004), in which reduction of cell flow velocity due to a single-beam trap crossing the channel was used to identify cancerous and non-cancerous cells by time-of-flight, with detection through scattering from a probe laser beam.

Tightly-focussed single beam traps are particularly suited to subwavelength particles (Svoboda and Block 1994) and have been exploited for the study of the scattering spectra of individual trapped silver nanoparticles of order 100 nm diameter, yielding information on their morphology-dependent resonances (Prikulis et al. 2004). An array of single beam traps generated using a VCSEL array was used to optically capture and manipulate in three dimensions a 2×2 array of red blood cells, and independently release them (Flynn et al. 2002). Further biological applications of this system are described by Ozkan et al. (2003), where two implementations of optical diversion of polystyrene microspheres between two outputs of a microfluidic junction under electro-osmotic flow are demonstrated, using the scattering force or the gradient force, respectively. Wang et al. (2005) then built upon the latter and demonstrated optical switching in a microfluidic fluorescence-activated cell sorter (FACS) citing improved buffer medium compatibility when compared with electrokinetic and dielectrophoretic methods. Throughput of GFP-expressing HeLa cells was up to 100 cells/s and recovery rates were >85%. No evidence of cell stress was observed in the recovered populations.

Stable trapping is particularly important when acquiring weak signals such as Raman spectra, as it allows improved noise reduction. Ramser et al. (2005) employed a single beam trap in an electro-osmotically controlled microfluidic system to observe Raman spectra of individual erythrocytes during the oxygenation cycle. The trapping beam entered from one side of the flow channel, while the Raman excitation and collection was configured on the opposite side of the channel, as shown in Fig. 2, allowing independent optimisation. The oxygenation cycle was clearly observed, but the high-intensity trapping illumination at a wavelength of 1,064 nm was observed to accelerate transfer of Hb to metHb, and lack of this deleterious effect at a trapping wavelength of 830 nm was noted. Neuman et al. (1999) conducted detailed multiwavelength measurements and showed that wavelengths of 830 and 970 nm are preferred for minimising cell damage. Buican et al. (1987) noted that a counterpropagating dual-beam trap may be preferred over the single-beam trap in practical cell manipulation, and this was emphasised by Jess et al. (2006) who realised a dual beam fibre trap [first demonstrated by Constable et al. (1993)] for Raman spectroscopy of cells in a simple microfluidic system, yielding localised Raman spectra from within primary trapped human keratinocites. The divergent fields result in a large area trap and allow large objects such as cells to be held and manipulated with greater positional control and reduced risk of photodamage when compared with conventional optical tweezers. An elegant application of a dual beam fibre trap to study the deformability of cells as a new biological marker for disease was demonstrated by Guck et al. (2005), and is illustrated in Fig. 3. The trap captures a cell in a microflow channel, centres it in the channel, and stretches the cell towards the opposing fibres to an extent dependent upon the incident power. The power dependent deformation, observed on a CCD camera, depends upon the cell rigidity, and may be used to distinguish between normal and cancerous human breast epithelial cells, for example.

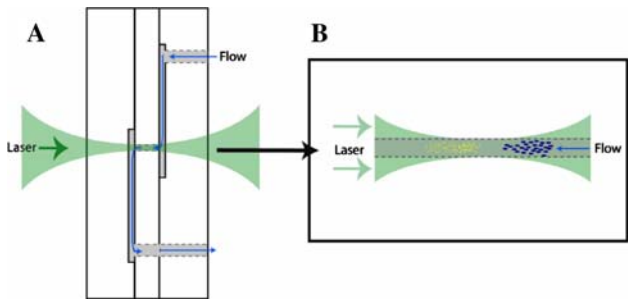

Fig. 1 Optical chromatography glass micro-flowcell; **a** construction of the microfluidic device showing the pathway for fluid and the laser beam focused on the channel, **b** illustration of a separation, in which sample particles are constrained to the focal point of the beam by the size of the separation channel that is filled by the laser beam (Hart et al. 2007). Reproduced with permission from the Optical Society of America

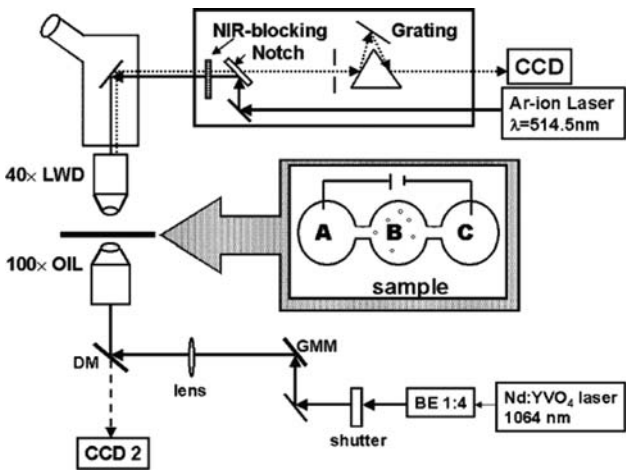

Fig. 2 Schematic of the experimental apparatus where a Raman spectrometer is combined with the optical tweezers in a double-microscope configuration (Ramser et al. 2005). Reproduced with permission from the Royal Society of Chemistry

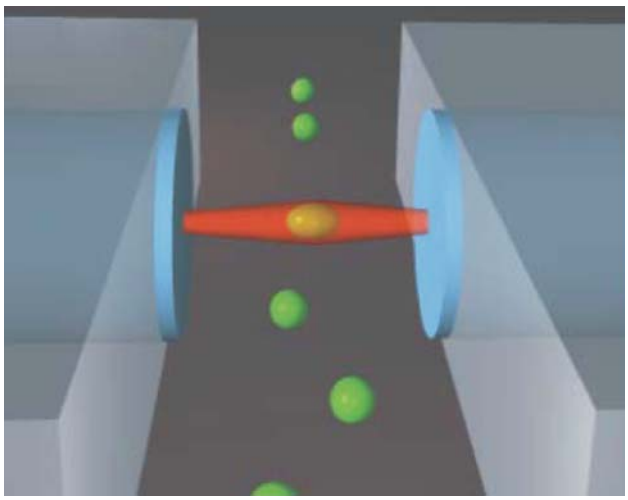

Fig. 3 Optically induced surface forces leading to trapping and stretching of cells (Guck et al. 2005). Reproduced with permission from Biophysical Society

2.2 Two-dimensional separation

A 100-μm long line-trap, rather than a point trap, has been generated by focussing a diode laser bar in a microflow channel (Applegate et al. 2004). Bovine red blood cells were captured by the line trap, which was placed at an angle to the flow direction, and the cells were conveyed along it before being released at its end, thereby deflecting cells of a certain size; time-dependent interruption of the beam may be used to sort cells into different fluidic output channels. Subsequently, optical waveguides written into a block of fused silica placed under the microfluidic system were used to excite fluorescence in line-trapped dye-doped polystyrene microspheres, allowing fluorescent-based activation of sorting (Applegate et al. 2006). The use of a potential landscape or optical lattice (Korda et al. 2002; MacDonald et al. 2003), where interference produces an array of traps has been employed to selectively deflect monodisperse 2 μm protein microcapsules from a externally pumped stream of polydisperse particles, and to sort erythrocytes from lymphocytes, in a simple microflow system (MacDonald et al. 2004). This approach has the advantage of flexibility in tailoring the potential barriers and thus the interconnection of traps for particle sorting. Paterson et al. (2005) observed that the requirement for external pumping of the fluid could be removed by breaking the symmetry of the lattice, for example by tilting the potential, and Milne et al. (2007) demonstrated simultaneous separation of four sizes of silica sphere between 2 and 7 μm into parallel output flows using an acousto-optically generated potential landscape, demonstrating simple programmable reconfigurability of the landscape. Further approaches to deflecting particles dependent upon their optical properties include the use of a composite microlens array to form a linear array of "optical rods" across a 2-D flow plane (Sun et al. 2006b).

2.3 Monolithic integration of lasers

Integration of waveguides from which light emerges into a microfluidic channel is an attractive advance upon the use of external lenses or the hybrid integration of individual optical fibres to realise dual-beam traps, in terms of robustness, alignment and potential for mass production. Cran-McGreehin et al. (2006a, b) demonstrated integration of semiconductor lasers emitting directly into a microfluidic channel, as shown in Fig. 4, to realise two dual-beam traps and demonstrate trapping of polymer spheres and shunting of these spheres between traps. The device was realised in a GaAs/AlGaAs heterostructure with InAs quantum dots emitting at 1290 nm, with microflow channel realised using chemically assisted ion-beam etching. This approach provides the potential for monolithic integration of all the optics and fluidics in highly functional devices, and potentially removes the need for any optical connection to the chip, which is often the most difficult aspect particularly for users not specialised in optics.

2.4 Evanescent field trapping and propulsion

Propulsion of particles in an evanescent field was demonstrated by Kawata and Sugiura (1992), where light incident on the base of a prism beyond the critical angle resulting in an evanescent field in water was used to propel polystyrene and glass spheres of diameter between 1 and 27 μm at velocities up to 20 μm/s along the surface of the prism. The evanescent approach allows convenient manipulation at a surface, improved stability as the radiation does not propagate through the liquid medium and, with the use of appropriate apertures, greater spatial localisation through the near-field, but the fields are normally restricted to within a few hundred nanometres of the surface. Forces in an evanescent field were exploited by Garcés-Chávez et al. (2005) to guide and trap red blood cells over an area of order 1 mm^2. A grating of period 12 μm was imaged on the base of a prism and the cells assembled along the lines of high intensity and moved along them under radiation pressure. A counter-propagating beam with the same grating pattern was used to produce the same gradient force pattern but equal and opposite radiation pressure forces parallel to the surface, thereby producing stationary traps. Control of the relative beam powers was used to control the velocity of cells from stationary to about 1 μm/s. Mellor and Bain (2006) used a similar two-beam geometry without

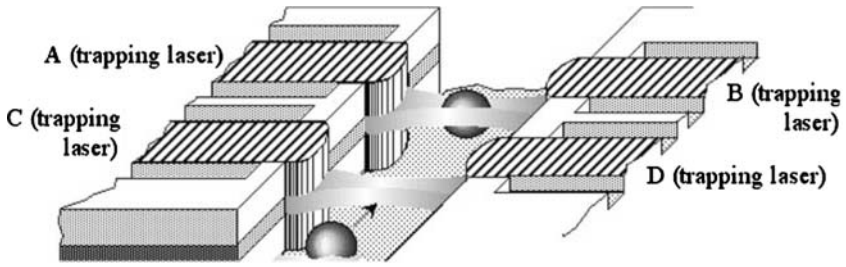

Fig. 4 Schematic diagram of monolithically integrated semiconductor laser traps (Cran-McGreehin et al. 2006). Reproduced with permission from the Optical Society of America

the grating image, and both with and without resulting interference fringes, to study the interplay of trapping and optical binding forces on collections of spheres of order 500 nm diameter to produce ordered arrays with controlled sphere spacings.

Optical waveguides provide evanescent fields and have the advantages of greater stability and potential for integration. Kawata and Tani (1996) demonstrated the trapping and propulsion of polystyrene latex and metallic spheres along a channel optical waveguide at velocities up to 14 μm/s, and suggested the use of a standing wave for positional control, and application to cell sorting according to "size, chemical composition and shape". Grujic et al. (2005) demonstrated optical sorting of 6-μm diameter polystyrene latex particles into the two output branches of a Y-junction glass waveguide, following external identification of the particles to be selected. Gaugiran et al. (2005) demonstrated increased propulsion velocity, using a high-index silicon nitride waveguide with a larger proportion of power carried in the evanescent field, and also demonstrated the trapping and propulsion of red blood cells and yeast cells at velocities up to 1 μm/s on these waveguides. Gold nanoparticles have a high scattering cross-section compared with latex particles and biological cells and have potential as tags in sorting of biological species. Hole et al. (2005) trapped and propelled 250 nm diameter gold spheres; individual particle trajectories exhibited velocities up to 500 μm/s, showing promise for high throughput sorting. Recently Schroll et al. (2007) have demonstrated bulk transport of liquid with mesoscopic spatial variations in refractive index under radiation pressure.

2.5 Optically driven micropumps

In addition to directly manipulating particles in microfluidic systems, there is a need for pumps and mixers to manipulate fluids themselves. While there are many demonstrations of pumps in microsystems, optically actuated pumps and mixers may have the advantages of simple reconfigurability, integration and small size, compared with external and piezo-electric pumps, and fewer constraints on the properties of the liquid medium compared to electrokinetic pumps. Colloidal particles, appropriately assembled into a microflow channel or chamber and manipulated using optical traps to provide pump action, are the most widely reported, with the two-lobe "gear pump" shown in Fig. 5 formed from four 3 μm particles, and a peristaltic pump formed from six such particles, being demonstrated by Terray et al. (2002). The particles comprising the pump were individually assembled and manipulated using scanning laser optical trapping, using a piezo-electric mirror under computer control to realise a time-averaged trapping pattern, with flow rates of 3 μm/s being achieved. Ladavac and Grier (2004) employed an array of ring traps, or optical vortices, formed by using a hologram to split laser light into two rows of three circular traps of few micron diameter; 800 nm silica spheres in the fluid were drawn into the rings and propelled around them by transfer of angular momentum. The helical phase functions for the optical modes driving the rings in the upper and lower rows were chosen such that their rotations were in opposite senses, so that the circulating rings of colloidal spheres caused the liquid between the rows to flow with velocities up to 5 μm/s. Leach et al. (2006) constructed a micropump by optically trapping two birefringent vaterite spheres of 6 μm diameter in a microflow channel and causing them to rotate in opposite directions, achieving a pump speed of up to 8 μm/s (200 fl/s). A single input beam was split using a Wollaston prism and waveplates to provide two traps with circular polarisation in opposite sense, imparting angular momentum to the spheres and causing them to rotate in opposite senses.

Rotation of a microgear with geometrical birefringence, using either circular polarisation to impart angular momentum or rotation of linear polarisation, in a conventional optical trap was demonstrated by Neale et al. (2005). The microgears, a few microns in diameter, were fabricated in SU-8 by e-beam lithography, released from their substrate, placed in the microflow system and positioned and rotated by the optical trap. Micropumps in which the rotors are fabricated around fixed shafts and rotated using optical forces have been demonstrated by Kelemen et al. (2006) and Maruo and Inoue (2006). Kelemen et al. incorporated an eccentrically positioned optical waveguide illuminating one side of the propeller to rotate it using scattering forces.

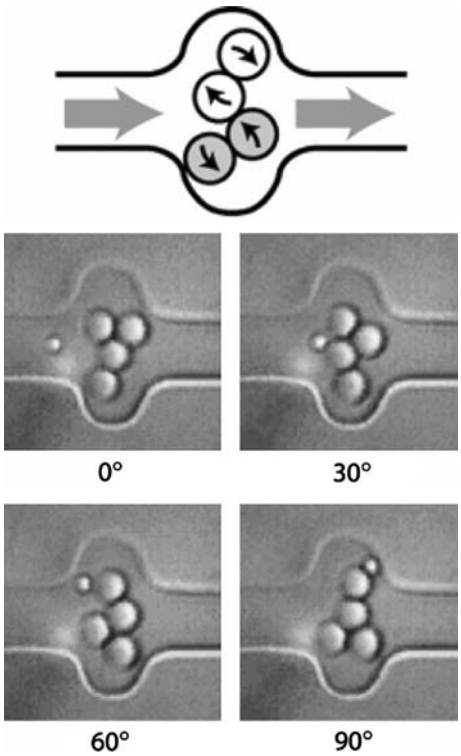

Fig. 5 Pump design illustrating lobe movement (the top pair rotate clockwise, the bottom counterclockwise) (Terray et al. 2002). Reproduced with permission from AAAS

All components were realised on a glass substrate by direct two-photon writing in photopolymers, and a rotation rate of 2 Hz was achieved with waveguide power of about 25 mW. Although reconfigurability is limited in this approach, as the propeller is "trapped" by an axle rather than by an optical trap, no complex external optics is required, the pump does not have to be assembled optically, and rotation is simply driven by waveguide power. Maruo and Inoue demonstrated a micropump shown in Fig. 6, with two counter-rotating meshing rotors in a protrusion in a 5 μm × 7 μm channel, rotating around fixed shafts, which achieved a pump rate up to 0.7 μm/s. All the structures were written by direct two-photon writing in photopolymer, and the rotors were driven by "time-divided laser scanning", dividing the beam and scanning the two resultant beams in opposite circular trajectories using galvano scanners.

3 Optical detection in microfluidic systems

Detection and analysis of chemical and biochemical species in microfluidic systems is challenging due to short optical path-lengths, small sample volumes, and the need to analyse individual particles or molecules. For the LoC to fulfil its potential in terms of parallelism and throughput,

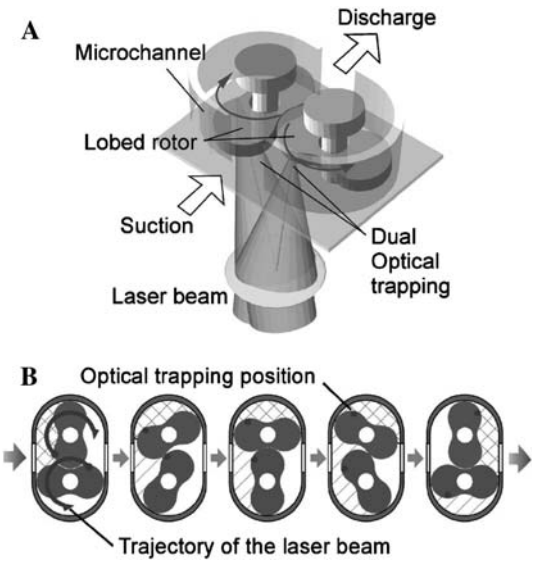

Fig. 6 Optically driven lobed micropump; **a** schematic diagram of the pump driven by time-divided laser scanning, **b** fluid transport by optically rotating two rotors (Maruo and Inoue 2006). Reproduced with permission from the American Institute of Physics

high-speed, multiparameter and multiplexed detection is required, creating heightened demand for low noise, high specificity, miniaturization and ruggedness. Conventional optical techniques for macro analysis such as fluorescence, absorption, and chemiluminescence have been applied to microfluidic systems, and recently good reviews have been published on optical detection methods for microfluidic devices (Götz and Karst 2007a; Yi et al. 2006b). Less common methods for optical detection in microfluidic devices, such as Raman spectroscopy, are reviewed by (Viskari and Landers 2006). The majority of optical detection systems in microfluidics address flow cytometry or capillary electrophoresis (CE). In common with demonstrations of optical trapping and propulsion in microsystems, most detection systems rely upon rather complex bulk-optical systems external to the microchannel, such as confocal microscopes, or hybrid integration by embedding optical fibres, rather than the full on-chip integration of optical functions likely to be required for highly functional integrated systems (Craighead 2006). While the majority of demonstrations use optical transmission directly through the fluidic channel, a few exploit evanescent field configurations where heterogeneous detection at a surface is carried out, exploiting the rapid diffusion to surfaces, which occurs in thin laminar flow channels. There are undoubtedly some challenges in applying evanescent sensing techniques, and integrated optical waveguides (Lambeck 2006), to microfluidic systems, such as the robustness and reversibility of chemically specific films and surface fouling, but biosensor research and microfluidics research appear artificially distinct at

present. This section reviews optical detection schemes for chemical analysis in microfluidic systems, divided according to the principal optical phenomena employed: scattering, absorption, refractive index, fluorescence, Raman spectroscopy, and thermal lensing. This review is limited to microfluidic systems, but there are many sophisticated optical systems which have been applied to biosensing and chemical analysis which use less advanced fluidics, but which have potential for future incorporation in the LoC.

3.1 Scattering

Light scattering techniques applied to collections of particles, such as turbidimetry, are well established, but microfluidics enables scattering measurements to be made on individual particles of size comparable with the wavelength, with high throughput. Scattering is probably the simplest method for cell counting in a microchannel, but can be extended to yield information on cell size, shape and internal and external structure according to the angular scattering spectrum, and is commonly combined with fluorescence measurements to yield chemically specific information. This is a natural extension of traditional bulk flow cytometry systems where scattering may be employed to increase detection reliability and the resolvability of fluorescent signals. Laser light is focussed on a detection volume and the scattering caused by a refractive index contrast between the particle entering that volume and the surrounding fluid allows detection of particles. Large angle scattering can give information a particle's surface roughness and internal structures; whilst small angle or forward scattering can yield information of a particle's size. Given the information which can be gained, scattering is surprisingly underutilised in microfluidic devices, perhaps due to the fact that most implementations are dependant on alignment of bulk external optics at the necessary angles.

Nevertheless, miniaturisations of flow cytometers using microfluidics have been developed, taking advantage of light scattering from particles. Schrum et al. (1999) used scattering from fluorescently labelled 2 μm diameter and unlabelled 1 μm diameter polystyrene latex particles to demonstrate flow cytometry in a microfluidic device, distinguishing them through fluorescence and size, and counting them at a rate of 13.5 Hz, using radiation from an Ar ion laser. Subsequently, McClain et al. (2001) extended this work to perform flow cytometry on fluorescently-labelled *E. coli* at a rate of up to 85 Hz, observing marginally better particle resolution using scattering. Witek et al. (2004) studied electromigration of *E. coli* and red blood cells in polymer microflow channels, using backscatter from focussed light from a 680 nm laser diode to monitor cell transport.

Pamme et al. (2003) analysed polystyrene microspheres of diameters between 1 and 9 μm in a microflow channel using scattering alone from incident light at a wavelength of 633 nm. Optical fibres to collect scattering were fixed externally on top of the microfluidic device at 15° and 45° to the incident light beam, as shown in Fig. 7. While particles between 3 and 9 μm diameter were readily distinguished at throughputs of order 150 Hz, the lower scattering intensities from smaller particles reduced the signal-to-noise ratio (SNR) to the point where 1 and 2 μm particles could not be reliably distinguished. The same group then analysed magnetic particles of diameter 2.8 and 4.5 μm under magnetophoretic separation. Similar apparatus was used as before but with scatter collection angles of 25° and 35° to the incident light (Pamme et al. 2006).

Wang et al. (2004) incorporated optical waveguides aligned photolithographically across the flow channel to perform scattering measurements on polystyrene microspheres of diameters 2.8, 4.6, 5.8 and 9.1 μm, avoiding the need for optical alignment and improving mechanical stability of the device. An integrated microlens was used to control the beam shape of incident light being delivered to the microchannel, and optical fibres were connected at the input and outputs. The channel, waveguides and lens were realised in a single SU-8 photoresist-processing step. Measurements of forward scattering were made by

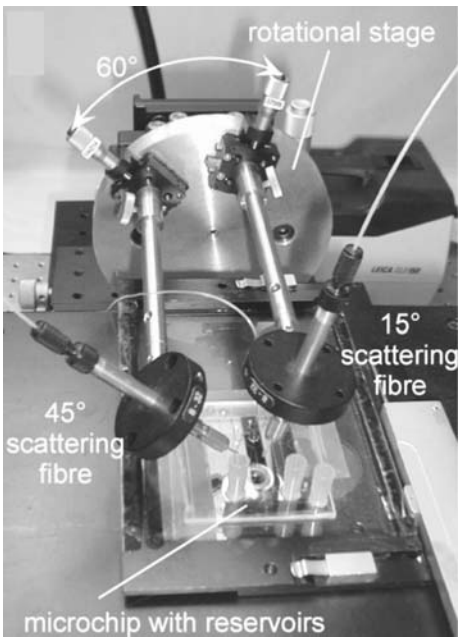

Fig. 7 Photograph of the microfluidic particle scattering apparatus; two optical fibres were mounted above the microchip for scattering detection. (Pamme et al. 2003). Reproduced with permission from the Royal Society of Chemistry

collection in an output waveguide at an angle of 5°, and the particles of different size were clearly distinguished. The design allowed for optical extinction and large-angle scattering to be measured, but this was not discussed in detail. Incorporating this approach in a dielectrophoresis structure the authors were subsequently able to separate and count viable and non-viable yeast cells (Wang et al. 2006). Integration of further components close to the scattering particles may be expected to yield more detailed information on cells.

3.2 Absorption detection

Detection through optical absorption is common in chemical analysis, employing either direct absorption in the UV/visible wavelength range or a colorimetric assay, for example. Its simplicity, and the lack of need for chemical derivitisations for fluorescent tagging, has led to it being the most widely used detection technique in conventional microseparations. However, the short optical path length inherent in miniaturization of fluidic channels leads to weak optical absorption competing with a high background transmission, and consequent difficulty in achieving low detection limits. This has been addressed in conventional capillary systems using Z-shaped and U-shaped channels (e.g. Moring et al. 1993) with longitudinal transmission. The problem becomes more severe in on-chip systems, and several approaches to increasing the absorption have been demonstrated, such as liquid-core waveguiding, multipass configurations, hollow prism cells, integrated waveguides and "slow light". Detection limit depends upon good stability and reduced noise as much as increased sensitivity, rendering waveguiding approaches attractive.

To enhance absorption in microfluidic devices, Liang et al. (1996) microfabricated a planar U-shaped absorption cell, with the base of the U placed between excitation and collection fibres in photolithographically defined channels, and achieved a 10-fold increase in absorbance, using a path length of 140 μm compared with transverse measurement through the 20 μm depth of the channel. Mogensen et al. (2001) integrated planar channel waveguides into a U-channel design for the coupling of light into the detection region, to overcome alignment issues observed with optical fibres, and used a larger optical path length of 750 μm, increasing this to 1,000 μm in a subsequent polymer device (Mogensen et al. 2003). They further increased this to an effective optical path length of 1.2 mm using novel pure silica integrated waveguides shown in Fig. 8 (Mogensen et al. 2004); using absorbance at a wavelength of 254 nm a detection limit of 3 μg ml^{-1} was achieved for paracetamol, and electrophoretic separation allowed caffeine, paracetamol, and ketoprofone to be distinguished. Launching and collecting light across long path-length channels has also been achieved using total internal reflection from micromachined V-grooves placed either side of the fluidic channel (Grumann et al. 2006) and used for a glucose assay on whole blood, where a limit of detection (LoD) of 200 μM was achieved.

Salimi-Moosavi et al. (2000) reported a multi-reflection cell, achieving five to tenfold enhancements of optical path lengths. Mortensen and Xiao (2007) have recently modeled the use of "slow light" structures for optical path-length enhancement. Periodic structures such as liquid-infiltrated photonic crystals could be incorporated within a flow channel and potentially yield large enhancements particularly near the band edges. Duggan et al. (2003) achieved an optical path length of 5 mm by using a Teflon fluoropolymer capillary as both the flow channel and a liquid-core waveguide, and Teflon AF coated waveguiding microflow channels in silicon have also been realised (Datta et al.

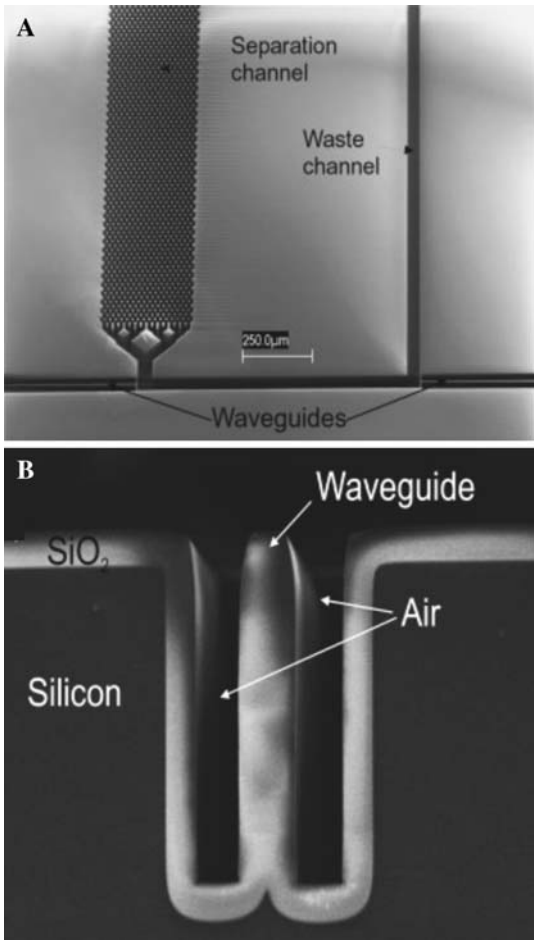

Fig. 8 **a** Scanning electron micrograph of the detection region of U-channel absorption device after etching and oxidation (*top view*). **b** Stripe of SiO_2 that acts as a waveguide (Mogensen et al. 2004). Reproduced with permission from Wiley-VCH Verlag GmbH & Co. KGaA

2003). However, extending the physical path-length along the direction of flow also degrades the spatial resolution of species in capillary separation systems, resulting in a trade-off between enhancement and resolution. Performance of absorbance based measurements can also be improved by incorporating additional on-chip optical components, such as microlenses and micro-apertures, to reduce stray light and hence increase the effective optical path length (Ro et al. 2005). Zhu et al. (2006) improved collection efficiency by incorporating bare silicon detectors within the PDMS fluidic chip and reported a LoD for bovine serum albumin of 1 μg ml^{-1} with channels of 60–400 μm depth. Llobera and co-workers developed monolithically integrated hollow prism microchannels combined with optical components in a single-step PDMS microfabrication process (Llobera et al. 2004, 2005). The device, shown schematically in Fig. 9, consisted of channels to embed input and output fibres and cylindrical biconvex microlenses to collimate the light, pass it through the hollow prism filled with analyte, reflecting from a prism wall to enhance path-length, and refocus it on the output fibre. LoDs of 1.83 and 0.683 μM were achieved for fluorescein and methyl orange, respectively, and pH measurements performed using methyl orange.

An alternative approach to overcoming the low UV absorptions obtained in microchannel separations due to the short optical path-length is to preconcentrate the sample. Isotachophoretic (ITP) preconcentration has been combined with zone electrophoresis (ZE) to lower the LoD on detection of two flavonoids down to 1.2 and 0.2 μg ml^{-1} (Ma et al. 2006), a 32-fold enhancement compared with zone electrophoresis alone.

Jiang and Pau (2007) fabricated an SU 8 rib waveguide in a PDMS microchannel with a spiral geometry resulting in a length of 110 mm within a chip area of 4 cm^2. The fluid to be sensed acts as a cladding and its spectroscopic properties are probed using the evanescent field. Hu et al. (2007) realised a chalcogenide glass waveguide in a PDMS microchannel, in principle allowing transmission and evanescent absorption spectroscopy at mid-IR wavelengths. Special waveguide designs can achieve higher sensitivity for evanescent detection than "free space" designs of the same physical path length (Veldhuis et al. 2000), rendering them potentially attractive in on-chip labs.

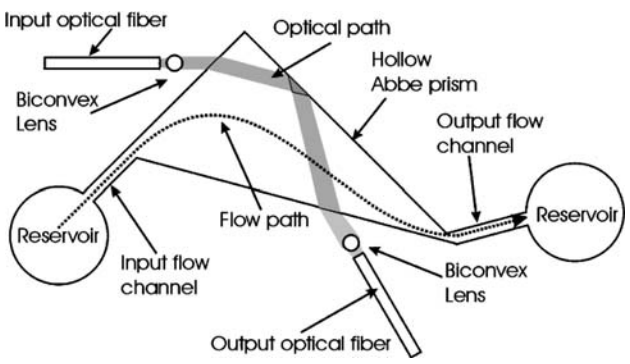

Fig. 9 Schematic of the system for detection with a hollow Abbe prism (Llobera et al. 2004). Reproduced with permission from the Royal Society of Chemistry

3.3 Fluorescence detection

Fluorescence techniques are by far the most commonly used for optical detection in microfluidic devices, having the prime advantage that the signal is usually readily separable from the scattered incident light. Compared to other detection techniques, fluorescence delivers high sensitivity, allowing detection of single molecules as reviewed by Dittrich and Manz (2005), and has gained wide acceptance in conventional bulk instruments. In some cases, the autofluorescence of species (molecules, viruses, cells, etc) may be detected; otherwise a fluorophore or quantum dot must be attached to act as a tag to be detected. Tagging has the disadvantage that additional sample preparation must be carried out, but usually yields lower fluorescent background and improved confidence in the measurement. Due to the vast literature on this topic, in this section only work published within the last 2 years will be discussed to highlight the most recent advances in applications of fluorescence in microfluidic systems.

A wide variety of light sources are used for excitation, including lasers, LEDs and lamps. Lasers and "laser-induced fluorescence" (LIF) are most commonly employed in microfluidics, due to diffraction-limited focussing and the potential for 2-photon excitation. The increasing range of wavelengths, continually reducing cost due to use in consumer electronics, good stability, ease of switching, and low power requirements when using semiconductor lasers reinforce this trend. Longer wavelength fluorophores (600 nm $< \lambda_{abs} <$ 800 nm) tend to be gaining ground due to the reduced background fluorescence and wider availability of high-quality compact optical components at these wavelengths.

Recent research has emphasised electrokinetic methods for concentrating species to be detected, thereby improving LoD, with most using conventional external optical apparatus such as confocal microscopes. It has been shown that field-amplified stacking injection (FASI) in microfluidic capillary electrophoresis devices can increase sensitivity of detection of fluorescent dyes (Gong et al. 2006). Using a microfluidic chip with several channel networks, detection of immunoassays of insulin secretions from multiple independent pancreatic islets can be continuously monitored with an LoD of 10 nM (Dishinger and Kennedy 2007). Sun and Yin (2006a) reported a multi-depth microfluidic device for single cell analysis. Human carcinoma

cells which tend to aggregate and settle were separated using this device and the cell constituents separated by CE and analysed using LIF. Flow cytometry is an important function to benefit from microfluidics technology, with many continuous-flow microfluidic devices demonstrating fluorescent-activated cell sorting (μFACS). Morgan and co-workers (Morgan et al. 2006; Holmes et al. 2006) reported devices that used dielectrophoresis (DEP) to focus particles in a microchannel stream. Figure 10 shows a micro flow cytometer chip, which focused particles in both the vertical and horizontal dimensions and detected 6 μm diameter fluorescent latex particles. Using careful optimisation of the excitation intensity to limit fluorophore saturation, Jung et al. (2007a) obtained an extremely low LoD of 100 attoM, and single molecule detection, of Alexa Fluor 488 by LIF in a CE chip flow with isotachophoretic separation. Hydrodynamic focussing has also been applied in microfluidic systems with fluorescence detection. Yang et al. (2006) realised a portable system incorporating a microfluidic device with hydrodynamic focussing and on-chip pumping and applied it to detection and sorting of fluorescent dye-labelled human lung cancer cells, with a count rate of 120 min^{-1} and an error rate better than 2%. Simonnet and Groisman (2006) created high-throughput flow cytometers (17,000 s^{-1}) in molded PDMS with "3D" hydrodynamic focussing, and applied them to tagged yeast cells. Kamei and Wada (2006) built upon earlier work (Kamei et al 2005) demonstrating microfluidic separation of biomolecules, and realised a detection platform shown in Fig. 11, which included a 2 mm diameter half-ball lens for fluorescence collection, a microstructured interference filter deposited directly on a pin photodiode, and an aperture through the centre of the detector and filter via which excitation light from a 488 nm frequency-doubled VCSEL was introduced. A planar microfluidic CE device was placed in contact with the half-ball lens, exciting fluorescein in the microchannel and allowing fluorescence to be collimated, filtered and collected. The device achieved an LoD of 7 nM fluorescein and was used to demonstrate the separation and detection of *Hae*III-digested øX174 bacteriophage DNA. Breakthrough of scattered excitation light is often the limiting factor in performance of fluorescence-based systems. Fu et al. (2006) performed a detailed study of the directionality of scattered excitation light and fluorescence, which enabled maximization of the fluorescent to scattered power ratio by selecting the fluorescence collection angle. Excitation light was incident orthogonally to the microfluidic substrate and collected in the plane of the substrate from the chip sidewall, as shown in Fig. 12, with angles of 45° and 135° to the flow-channel exhibiting the best performance. An LoD of 1.1 pM fluorescein was achieved, and the device demonstrated CE of tagged arginine and phenylalanine.

Waveguiding structures have been exploited for fluorescence-based detection in microfluidic systems. Mazurczyk et al. (2006) realised ion-exchanged waveguides in soda-lime glass integrated with etched microfluidic channels and used fibre-coupled laser light at 532 nm for excitation of the Cy3 dye. Collection was carried out orthogonally from the top of the chip using a lens or bonded fibre, achieving an LoD as low as 0.5 nM Cy3, and collinearly in a waveguide on the opposite side of the channel, achieving an LoD of 1 μM Cy3. The orthogonal configuration was then used to demonstrate CE of Cy3 and Cy3-tagged streptavidin. Bernini et al. (2006) used antiresonant reflecting optical waveguide (ARROW) structures to realise microfluidic channels that guided excitation light in the liquid, an alternative approach to the Teflon-clad waveguides described above. Although the liquid core has a lower refractive index than the surrounding media, the dual-layer cladding forms a high reflectivity mirror, which traps the light without invoking total internal reflection. Laser light was coupled into the flow channel via a fibre inserted into the hydrodynamically focused sample stream and two detector fibres were inserted in microchannels perpendicular to the main channel to capture fluorescent light from passing particles.

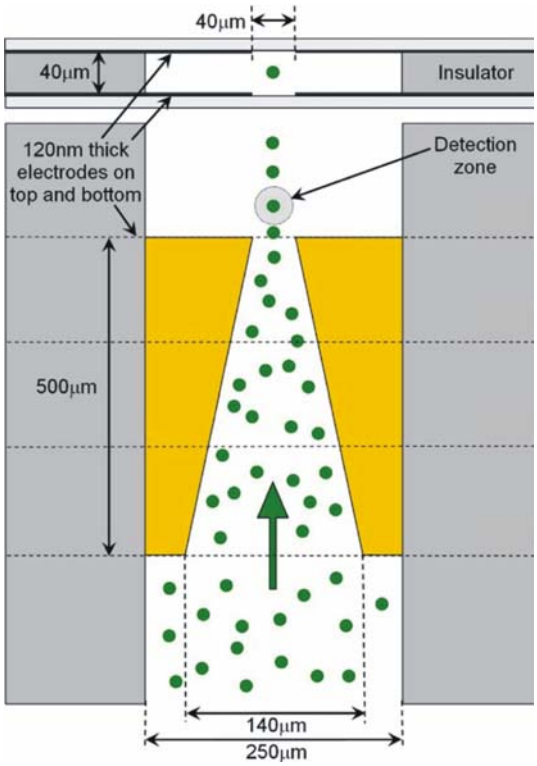

Fig. 10 Schematic diagram of flow cytometer chip, showing the four focussing electrodes in top–down and cross-sectional views and the position of the optical detection zone and how the particles are focussed into this region by the electrodes (Holmes et al. 2006). Reproduced with permission from Elsevier

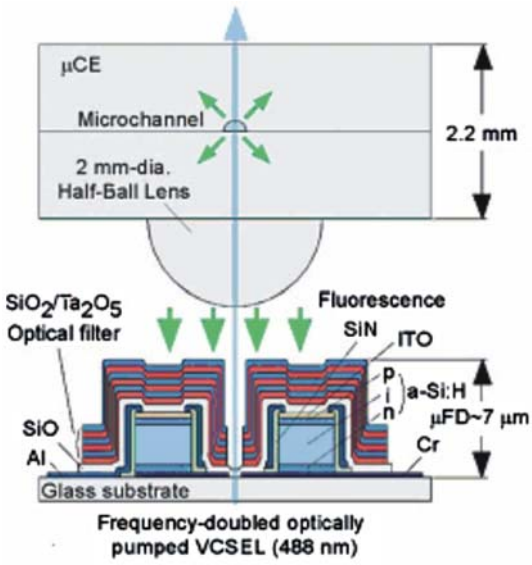

Fig. 11 Cross-sectional view of the fluorescence detection platform on which a capillary electrophoresis chip is mounted. Laser light is introduced from below through an aperture (Kamei and Wada 2006). Reproduced with permission from the American Institute of Physics

The system was tested with human T leukaemia cells with diameters of about 20 μm.

The rapid, low-cost, detection of bacteria in food and drink is an important application for micro flow cytometry. Small numbers of *Pseudomonas* cells in milk (Yamaguchi et al. 2006) and *E. coli* in buffer (Inatomi et al. 2006) were detected using fluorescence microscopy following attachment of fluorescent dyes. A more portable PDMS immunoassay system that detects the *E. coli* O157:H7 bacterial antigen with an LoD of 0.3 ng μl^{-1} has been reported (Xiang et al. 2006). A laser diode and optical fibre-based fluorescence excitation and collection module was employed, with the distal end of the multimode fibre placed against the bottom side of the thin glass fluidic substrate. Li et al. (2006) employed an optical fibre embedded in an etched channel in the substrate and a blue (470 nm) laser diode for detection of fluorescene-5-isothiocyanate (FITC)-tagged neurotransmitters dopamine and epinephrine in a micro CE chip.

Fluorescence correlation spectroscopy (FCS) is a powerful technique for the determination of the physical properties of small numbers of fluorescent or dye-tagged molecules. To ensure that only small numbers of molecules are studied at one time, the excitation volume is minimised by focussing to a small volume and using confocal detection. A correlation analysis of the temporal fluorescence fluctuations of particles entering the optical detection volume yields information on the diffusion characteristics and other physical properties of the molecules under study. Yeh et al. (2006) assembled an FCS system with a complex PDMS microfluidic network, consisting of on-chip serpentine channels for mixing, interrogation chambers, reservoirs and valves, as shown in Fig. 13. In a single flow-chip, the drug doxorubicin was mixed to produce eight parallel streams of different concentration; each stream was then mixed with a complex of DNA with transcription factor Sp1, and incubated in eight parallel interrogation chambers. Sp1-DNA dissociation was then determined by FCS, exploiting the different diffusion kinetics of differently sized entities to determine the fractions of bound and unbound DNA. The resultant dose-response titration curve yielded the Sp1-DNA binding inhibition versus drug concentration. Rapid detection of low numbers of viruses for medical diagnostics is an important field of application of microfluidics. Zhang et al. (2006) detected dengue virus with fluorescence cross-correlation spectroscopy (FCCS), using dengue-specific antibody in a PDMS microfluidic array structure. The virus and antibody were fluorescently labelled with two different fluorophores, excited at 488 and 633 nm, and the emission separated by a dichroic filter onto two APDs. Viruses bound to antibodies entering the detection volume exhibited positively cross-correlated

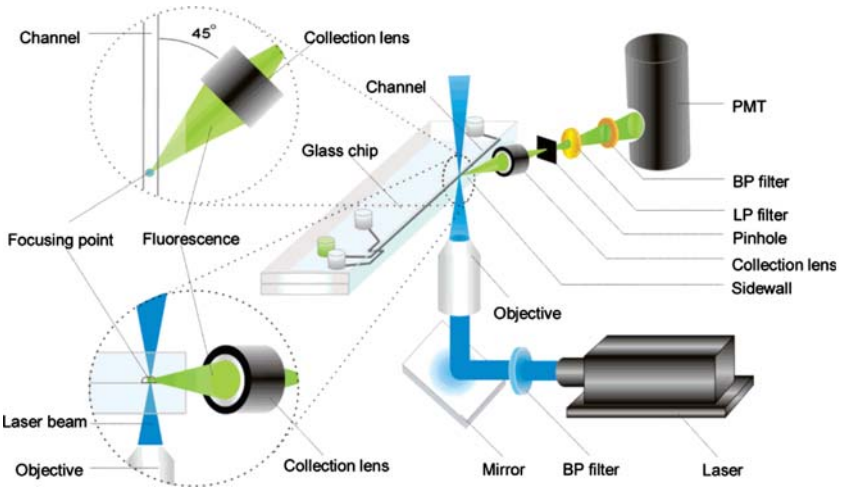

Fig. 12 Schematic diagram of angle-resolved fluorescence detection apparatus (Fu et al. 2006). Reproduced with permission from the American Chemical Society

fluorescence signals due to their motion being coupled. This study suggests that detection of a single virus is achievable with this system. Hollars et al. (2006) also performed a cross-correlation of two fluorescence labelled probes excited and emitting at different wavelengths, in a flowing system. In this case total internal reflection was used to excite the dye-tagged analyte in an evanescent field in the microchannel. Short non-amplified DNA sequences were measured to sub 100 pM levels in less than 1 min.

Advances have also been made in systems employing conventional lamps, which allow great flexibility in excitation wavelength by using wavelength filters, but generally show poorer limits of detection. Yan et al. (2006) used an Hg-lamp with excitation wavelengths from 300 to 600 nm and a carefully engineered detection system with a microfluidic CE chip to achieve an LoD for FITC of 7×10^{-10} M and for FITC-tagged cystine of 9.6 nM. Götz and Karst (2007b) used a xenon arc lamp as an excitation source combined with a spectrograph and CCD, providing more detailed information through the complete emission spectrum in the visible wavelength range (350–800 nm). Three rhodamine dyes were used to characterise the system, applied to a standard microfluidic chip performing CE for separation of analytes. Peaks in the elution spectra could be assigned to different pure analytes and unexpected impurities were detected both by CE separation and within an elution peak using spectral information. Using similar apparatus the group were then able to detect thiols found in cosmetics with an LoD of 2 μM (Revermann et al. 2007) and taurine found in drinks with concentrations as low as 60 aM (Götz et al. 2007c). Mitra et al. (2006) fabricated a microdischarge device stacked on top of a microfluidic device as an alternative excitation light source producing emission in the UV for intrinsic fluorescence excitation. The microdischarge is created in an air gap between a metal anode and saturated salt solution in a reservoir acting as a cathode.

Light-emitting diodes (LEDs) are attractive sources for microfluidic measurements as they are cheap, compact, and efficient and may have higher brightness than conventional lamps. Destandau et al. (2007) have reported a simple Y-shaped microfluidic channel and a simple LED and PMT detecting potassium with a LoD of 0.5 mM using calyx-bodipy dye, which has fluorescence intensity sensitive to potassium concentration. Kim et al. (2006) realised a highly integrated fluorescent microfluidic detection chip comprising the microfluidic channels, silicon detector with interference filter, and an integrated organic LED (OLED) deposited directly on to glass as a thin-film structure. The microchannels were etched in glass with dimensions 70 μm width and 20 μm depth, and the OLED, emitting at 530 nm, was deposited on the reverse of the substrate. A p-i-n photodiode with a deposited interference filter was buried in PDMS, which was then bonded to the glass microchannel. The device was characterised using tetramethylrhodamine dye (TAMRA) and achieved an LoD of 10 μM. Hofmann et al. (2006) realised microchannels in a PDMS slab, which had been doped with lysochrome dye and acted as a high-quality filter itself. 1 mm thick samples doped with 1,200 μg ml^{-1} Sudan II, for example, showed <0.01% transmission at 500 nm and >80% transmission above 570 nm. Irawan et al. (2006) realised microchannels for use as fluorescence detection cells in PMMA optical fibre and plastic clad silica optical fibre by laser ablation. Microchannels of dimension 100 μm width by 210 μm depth were etched into the fibre cores and fluorescein, excited by a blue LED (centre wavelength at 470 nm), measured with an LoD of 5 ng l^{-1}.

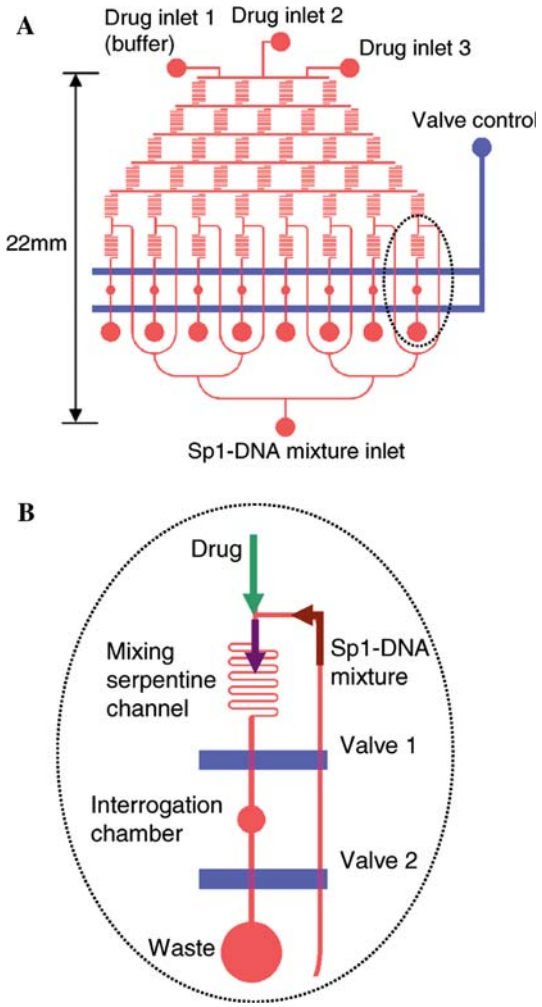

Fig. 13 The PDMS-based microfluidic chip used for investigation of the dissociation of Sp1–DNA complex by DOX. **a** The layout of microchannels (*red*) and the mechanical on-off valves (*blue*). **b** A zoom-in of the mixing portion on the microfluidic chip (Yeh et al. 2006). Reproduced with permission from Oxford University Press

Protein and DNA detection and manipulation are major fields of application in microfluidic systems due to the

benefits of rapidity, flow control and small sample and reagent volumes at these scales. Shen et al. (2006) developed an array of CE microchannels connected to reservoirs in soda-lime glass to perform parallel detection of fluorescent-tagged biomolecules. Light from a diode-pumped solid-state laser at 473 nm was line-focussed across the parallel measurement and reference channels and a CCD camera with filter was used to detect fluorescence simultaneously from all channels. Parallel CE separation allowed simultaneous detection of many fluorescently labelled molecules such as amino acids, proteins and nucleic acids. A similar system was realised in PMMA by Liu et al. (2006), working in the same group, and successfully applied to rapid detection of multiplex PCR products for SARS and hepatitis B. Huang et al. (2007) fabricated a sophisticated microfluidic network in PDMS to analyse low-copy number proteins in a single cell by single molecule detection. Individual cells were trapped, lysed, and the proteins in the lysate bound with fluorescently labelled antibodies and then separated using CE. A line-focused laser beam ensured that all molecules across the width and depth of the detection microchannel (40 μm × 1.8 μm) were detected, while in the direction of flow it was still tightly focussed to reduce background fluorescence. Edgar et al. (2006) performed detection of fluorescein-labelled amino acids contained in 10 fl droplets. The device consisted of a T-channel 3 μm wide by 3 μm deep that separates a CE channel (50 μm wide by 50 μm deep) from the droplet generation input by using an immiscible liquid. LIF is then performed in the CE channel. Oh et al. (2006) genetically engineered *E. coli* cells to cause them to express capture proteins and present them at the membrane surface. DEP cell traps were used to immobilise the cells in 200 μm wide microchannels, which then captured fluorescently labelled target molecules. Dual wavelength fluorescence measurements were performed on the cells to detect the bound molecules and reference to the number of capture ligands. This technique provides a convenient method to produce surfaces with immobilised capture molecules. Direct UV-excited fluorescence offers the potential for label-free protein analysis in individual cells. Hellmich et al. (2006) performed direct UV fluorescence measurements on amino acids and proteins, using a frequency-quadrupled Nd:YAG laser and photomultiplier. Individual cells were optically trapped and electrically lysed on an PDMS/quartz chip, and the lysate separated by CE. Optimisation of the confocal optics and addition of carbon black into the PDMS led to a reduction in background florescence and an LoD of 25 nM for tryptophan.

DNA hybridisation to a free DNA probe sequence in solution is much faster than to immobilised DNA sequences, due to the diffusion-limited kinetics of the latter. Thus detection of hybridisation of target and probe in a microflow system, with suitable mixing, presents considerable advantages in terms of speed. Lee and co-workers (Yea et al. 2006; Kim et al. 2007) implemented a fluorescence resonance energy transfer (FRET) system in a PDMS microfluidic device with an "alligator teeth" structure for efficient mixing in otherwise laminar flow, shown in Fig. 14b. As the probe and hybridised target is not immobilised, washing cannot be used to remove the unbound target, so an alternative labelling scheme is required. Yea et al. (2006) employed a system where both the target DNA and probe strands were labelled, and relative intensities yielded the fraction of hybridised DNA. To avoid the need to label the target DNA, Kim et al (2007) then employed a molecular beacon, shown in Fig. 14a, where one end of a single-stranded oligonucleotide has a fluorophore attached and the other end has a quencher attached. In the absence of the target sequence, emission is quenched as the probe sequence forms a loop and the fluorophore and quencher are in close proximity. Hybridisation of the complementary target causes the loop to open, the fluorophore and quencher to separate and fluorescence to be observed. Liu et al. (2007) report a portable genetic analysis system for forensic applications and have validated it using samples extracted from oral swabs and human bone extracts. The glass microfluidic chip performed the polymerase chain reaction (PCR) and capillary electrophoresis followed by parallel four-wavelength fluorescence detection using a 488 nm frequency-doubled diode laser and confocal optics, with optical fibre as confocal aperture.

Multiplexed analysis with multiple fluorescent labels is limited by the spectral overlap of fluorophore emission. Pregibon et al. (2007) created single and multi probe particles encoded with a spatial fluorescent pattern for multiplexed detection of DNA oligomers at 500 attomoles. The encoded particles were created in a continuous microflow system, shown in Fig. 15a, where laminar fluorescently labelled monomer and probe-labelled monomer flows are introduced adjacently. Elongated polymer particles (∼90 μm wide by 30 μm deep by up to 270 μm long) were formed in the channel by exposing the monomers to 30 ms bursts of UV to photopolymerise them. The shape of the particles was defined by a mask in the UV projection system, which included the 20-dot pattern at one end, yielding more than one million possible codes. The resultant particles, which have a fluorescent graphically encoded region and covalently coupled probe-carrying regions, as shown in Fig. 15b, are collected in a reservoir. After incubation with the fluorescent-labelled target the particles are read by passing them through a microfluidic channel a little wider than the particle width. The particles are hydrodynamically focused and aligned along the channel and when they pass through the detection region the fluorescent intensities are detected using a CCD camera

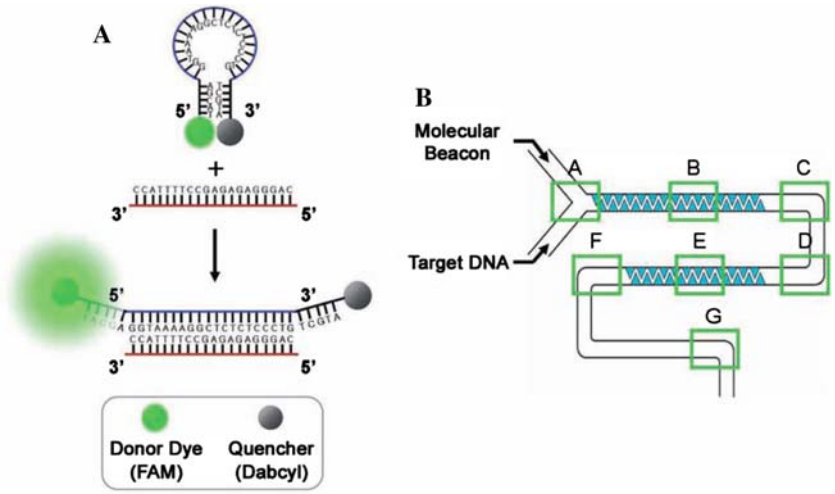

Fig. 14 **a** Schematic representation of the molecular beacon and its operating principle. Target hybridization leads to the separation of the fluorophore (*FAM*) and quencher (DABCYL) and a consequent fluorescent signal. **b** Schematic representation of an alligator-teeth-shaped PDMS microfluidic channel (Kim et al. 2007). Reproduced with permission from the Japanese Society for Analytical Chemistry

and analysed in five "lanes" along the particles, corresponding to the rows of dots in the code, so that the particle's code is read and the presence of the target is detected. The external optics employed in microfluidic LIF systems is often complex. Huang et al. (2006a) performed on-chip PCR and CE in PDMS/PMMA/glass multilayer device with an embedded optical fibre for fluorescence collection to reduce the complexity of collection. They detected *S. pneumoniae* bacteria and the dengue-2 virus by separating and detecting amplified DNA products.

Suitably modified microbeads may be used as probes for biomolecular detection in microfluidic systems. For example, the beads may be functionalised with antibodies and binding of the fluorescent-tagged antigen enables fluorescent detection in a microfluidic device, with multiplexing being achieved using beads containing different fluorophores. Detection on beads means that the antibody does not have to be immobilised in the microfluidic device, and the beads can be readily manipulated within a microflow system. Yun et al. (2006) realised physical PDMS gate valves within a microfluidic channel to isolate individual beads, as shown in Fig. 16. Using 10 μm diameter polystyrene beads modified with human IgG specifically bound to protein A on the bead surface, an LoD of 0.1 μg ml^{-1} for anti-human IgG conjugated with CdSe/ZnS quantum dots (QDs) was achieved, using a fluorescence microscope to excite and detect. Riegger et al. (2006) performed sandwich immunoassays for hepatitis A and tetanus in a centrifugally propelled disk-based microfluidic system with an LED light source. CdSe QDs were used to identify the beads and fluorescent polystyrene microspheres were used to identify presence of the bound antigen. Haes et al. (2006) achieved an LoD of 1 fM for *Staphylococcal enterotoxin B* (SEB) detection using a microfluidic device with a system of microchannels and micro-weirs. Displacement assays were carried out on a glass chip using LIF and electrokinetic fluid pumping. Silica beads modified with antibodies specific to SEB were trapped in the weirs, and fluorescent-tagged SEB bound to these in situ. The displacement assay was carried out by introducing the sample containing SEB and observing fluorescence from displaced tagged SEB downstream from the beads. The beads could be replaced, for repeated assay, or used again a limited number of times.

3.4 Refractive index techniques

Refractive index based techniques are more prone to influence by non-specific effects than fluorescence techniques but are extremely attractive for chemical and biochemical sensing due to the lack of need for a label. However, rather few papers describe integration of refractive index based detection techniques with true microfluidic systems, and key examples are reviewed in this section.

Costin et al. (2003) demonstrated measurement of diffusion coefficients and molecular masses in a microfluidic chip, which could play a useful role in on-chip CE and HPLC systems. The sample stream and mobile phase stream were merged in a detection channel and interdiffusion between the streams was monitored using the angular deflection of laser light by the resultant refractive index gradient. Two detection points, one just as the streams merge and one downstream, were used to monitor the extent of diffusion over the length of the channel, and the relative deflections yielded information on analyte diffusion coefficient and molecular weight. Leung et al. (2004) analysed bubbles in microchannels 40 μm wide and 30 μm deep, for application in on-line reaction monitoring and safety applications. As a bubble passes through the microchannel the deflection of laser light due to the

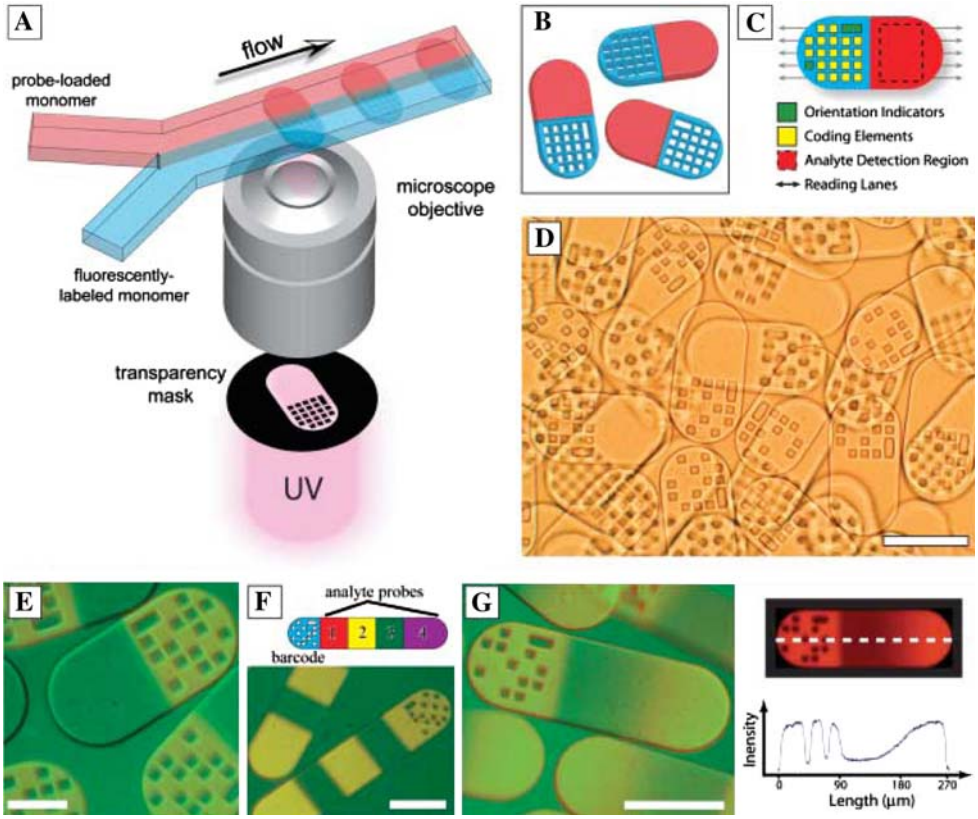

Fig. 15 **a** Schematic diagram of dot-coded particle synthesis showing polymerization across two adjacent laminar streams to make single-probe, half-fluorescent particles (shown in **b**). **c** Diagrammatic representation of particle features for encoding and analyte detection. **d** Differential interference contrast (*DIC*) image of particles generated by using the scheme shown in **a**. **e** to **g** Overlap of fluorescence and DIC images of single-probe (**e**), multiprobe (**f**, *bottom*), and probe-gradient (**g**, *left*) encoded particles. *Scale bars* indicate 100 mm in (**d**), (**f**), and (**g**) and 50 mm in (**e**) (Pregibon et al. 2007). Reproduced with permission from AAAS

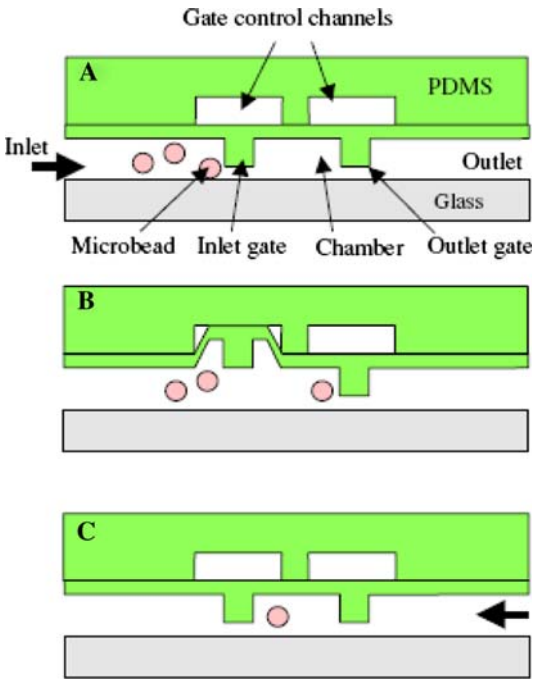

Fig. 16 Schematic view of each step in capturing of a single microbead: **a** bead introduction, **b** inlet gate opens by applying a vacuum to the gate control channel and **c** gate closed by stopping the vacuum on the gate control channel resulting in a single bead captured for sensing (Yun et al. 2006). Reproduced with permission from the Institute of Physics

refractive index perturbation is recorded using a position-sensitive detector. Performing statistical analysis on the data the system is able to determine bubble size and formation frequency. Using a hollow Abbe prism as a microfluidic chamber, as described above for absorption monitoring (Fig. 9), Llobera et al. (2004) were able to detect changes in refractive index through dispersion of the prism, as well as the absorption of a liquid. The device consisted of channels to embed input and output fibres, biconvex microlenses to focus the light, reservoirs, and the Abbe prism monolithically integrated in PDMS.

The spectral transmission of a Fabry–Perot cavity is highly sensitive to intracavity refractive index and may enable imaging of refractive index distributions. Shao et al. (2006) fabricated a Fabry–Perot (FP) microfluidic cavity in which microchannels of up to 30 μm deep and 200 μm wide were etched in Pyrex and the top and bottom coated with 35 nm thick gold layers to serve as reflectors. Using an LED as a broadband source and measuring the transmission spectrum of the device, they performed intracavity measurements on single particles such as yeast cells; human red and white blood cells could be distinguished, although improved quantification is needed. Song et al. (2006) realised a microfluidic network incorporating a dual-fibre Fabry–Perot, with channels for insertion of cells and two buffer solutions, two single mode fibres with high reflectivity gold-coated ends crossing the fluid channel to

act as the FP cavity and as optical input and output, and a pressure-based cell-holder to trap the cell between the two fibres, as shown in Fig. 17. The cavity was 35.5 μm long and two buffer solutions having different refractive indices were alternated while the cell was trapped in position by the cell holder. The differences in the spectra with the two buffer media were reported to yield the effective refractive index of the cell with a standard deviation of ±0.2%, and cell size with an SD of ±4% for repeated measurements of the same cell, being released and retrapped.

There is a vast literature on evanescent wave refractive index based biosensing, based on dielectric waveguides or on surface plasmon resonance, for instance, and these are subject of excellent recent reviews by Lambeck (2006) and Phillips and Cheng (2007). Integration of these sensors with microfluidic circuits is essential for repeatable performance, integration of reference sensors, enhanced interaction of analyte and surface, and low-cost manufacture, and the LoC may benefit greatly from these well-developed techniques. Mach-Zehnder interferometers (MZIs) are one of the most sensitive waveguide devices for evanescent refractive index measurement (Quigley et al. 1999), particularly if active electro-optic control is employed (Heideman and Lambeck 1999). Lechuga and co-workers have reported the development of an MZI using CMOS compatible technology integrated with an SU-8 microfluidic channel (Blanco et al. 2006; Sepúlveda et al. 2006), achieving an LoD for bulk refractive index of 3.8×10^{-6}.

Ymeti et al. (2005) realised a waveguiding Young interferometer (YI) on silicon with a glass microfluidic circuit. Light is inserted into a waveguide and is split into four channels. The outputs of the four waveguides are focused by a cylindrical lens to a CCD camera to record the interference pattern. Each of the four-waveguide channels is exposed in a sensing window, and microfluidic channels

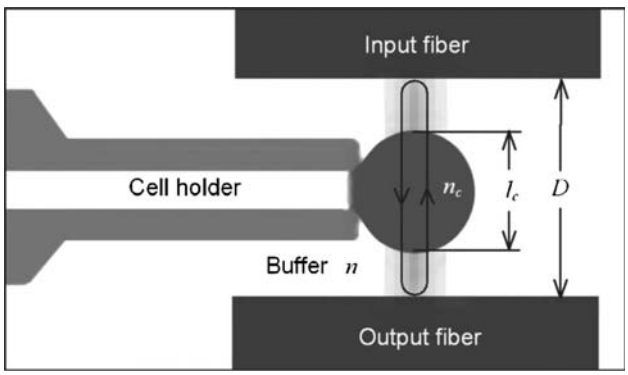

Fig. 17 Schematic showing microfluidic Fabry–Pérot cavity for cell detection. The cell holder holds a cell in position as the cavity resonates (Song et al. 2006). Reproduced with permission from the American Institute of Physics

are realised on a separate wafer, which is then bonded to the YI over the sensing windows. The device was used to analyse an immunoreaction between human serum albumin (HSA) and α-HSA and achieved a refractive index resolution of 6×10^{-8}. The authors later reported that a similar YI device, shown in Fig. 18, could detect herpes simplex virus type 1 (HSV-1) at concentrations of 850 particles ml^{-1} and that the sensor may be able to achieve sufficient sensitivity to detect single virus binding (Ymeti et al. 2007). In this case, a macrofluidic flow system was used, but the use of microfluidics was predicted to reduce the sample volume to a few microlitres and reduce time response to seconds.

Gratings are attractive components for interrogation of refractive index in microfluidic systems, as they allow relaxed optical alignment compared with direct end-coupling into waveguides (Duveneck et al. 2002). Yuen et al. (2005) realised a polymer H-shaped microfluidic device integrated with a grating for sensing, in which a reference fluid and analyte fluid could be passed over the grating under the same conditions and measured simultaneously. Laser light is incident through a polariser and focused via a lens to provide many angles to couple into the grating. Light is coupled into the waveguide at the angle where the grating provides phase matching, and this angle changes depending on the refractive index of the material at the grating surface; the light then couples out of the waveguide and is recorded by a CCD camera. Tests with biotin/streptavidin assays were conducted to demonstrate detection of small molecule binding. Sarov et al. (2006) employed a grating realised with a PMMA microprism on a glass microchannel lid, requiring multi-step fabrication. Laser light enters the prism under total internal reflection, so that the grating is irradiated and an evanescent field penetrates the microchannel. Reflected and diffracted light exits the prism and the energy redistribution into the diffracted orders allows the determination of the refractive index and the absorption coefficient of the fluid. The device had an index sensitivity of 5×10^{-4} and an absorption coefficient sensitivity of $3.5 \times 10^{6}\ m^{-1}$. Choi and Cunningham (2006) fabricated grating structures with a period of 550 nm as the sensors on the floor of a microchannel, by molding followed by deposition of a thin titania film. Using a white light source the grating is irradiated perpendicular to the grating with polarised light, and the reflected light, whose wavelength depends strongly on the refractive index of the medium in contact with the grating, is directed back to an imaging spectrometer. The key advantage of this approach is that an array of small sensor patches ($\sim 10 \times 10$ μm) can be imaged as independent sensors, allowing the potential for dense integration. The device detects changes of refractive index in the microchannel as a shift in the peak wavelength of reflection. Discrimination

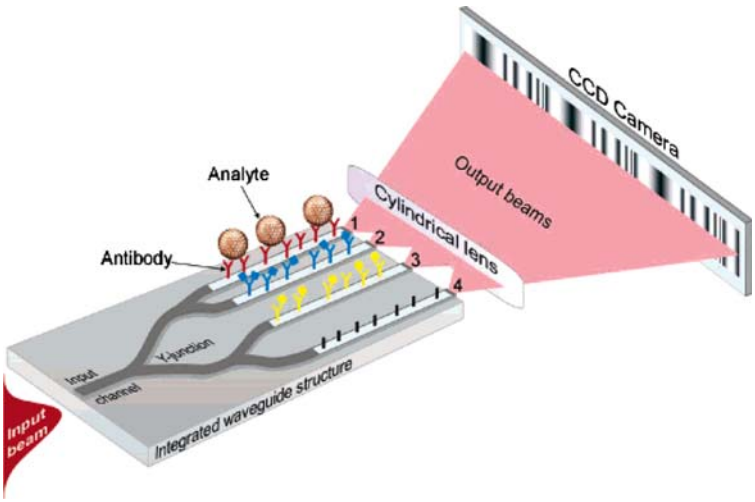

Fig. 18 Four-waveguide integrated optical Young's interferometer sensor. Waveguides 1, 2, and 3 are sensing arms, and waveguide 4 is the reference arm (Ymeti et al. 2007). Reproduced with permission from the American Chemical Society

between chicken IgG and pig IgG was demonstrated using Protein A as the immobilised protein ligand.

Surface plasmon resonance is an alternative means of detecting refractive index changes in an evanescent field, which has achieved great success through the Biacore™ system (Malmqvist 1993). Detection depends upon angle- or wavelength-dependent coupling to a lossy surface plasma wave at a metal surface, whose velocity changes with refractive index resulting in a change in reflected power. The potential for low reagent and sample volumes and fast reactions is driving further miniaturization and integration of SPR devices in microfluidic systems. Furuki et al. (2001) realised photopatterned microchannels with floors coated with a gold film. The device was excited using a prism in the Kretschmann configuration where light is reflected from the 60 nm thick gold layer, tunneling through it to excite a surface plasmon on the liquid side of the film in each channel. A sequence of cysteamine, photobiotin, and avidin was bound to the surface and measured by SPR. The results were consistent with those measured by atomic force microscopy, and the channel sample volume was reduced to about 8 nl. Wheeler et al. (2004) fabricated micro-flow cells designed to be attached to the commercial Spreeta™ SPR sensor by soft lithography in PDMS using conventional photoresist processing. Refractive index changes due to biotinylated bovine serum albumin, streptavidin, biotinylated protein A, and human immunoglobulin each bound to the preceding layer were monitored. Using volumes as low as 73 nl, the data were consistent those obtained with conventional flow cells of volume 8 µl. Recently more sophisticated microfluidic SPR devices have been reported. Huang et al. (2006b) realised a complex integrated flow circuit with many microfluidic components, and detection regions for three analytes in one channel. The optical excitation and detection was again achieved using an external prism in the Kretschmann configuration. Temperature control was incorporated into the device, as all refractive index based sensors are sensitive to temperature variations. Molecular imprinted polymer (MIP) films were used as the recognition element for specific biomolecules. MIPs specific to testosterone, cholesterol, and progesterone were pattered on the gold and detection of these three analytes successfully demonstrated at physiologically normal concentrations. This microfluidic SPR system demonstrated direct detection of low molecular weight analytes, higher association rates between analyte and MIP compared with a conventional SPR system due to more efficient interaction between biomolecules and MIP films, and reduced sample consumption.

Lei et al. (2007) integrated a microfluidic vortex pump into a hot embossed PMMA micro flow cell, with integrated SPR sensor. The gold layer was not deposited directly in the microchannel, but on the surface of a prism attached to an open microchannel, thereby sealing it. The sensitivity of the SPR technique was enhanced by exploiting the phase change on reflection as well as the amplitude change, in a bulk interferometer. An estimated sensitivity of $\sim$10 ng ml^{-1} was achieved for the binding reaction of BSA antibodies to BSA immobilised molecules on the gold surface. Making use of a simple T-shaped PDMS microchannel on a glass wafer with gold patches, Kurita et al. (2006) realised a portable SPR system with a concentration range of 5 pg ml^{-1} to 100 ng ml^{-1} for B-type natriuretic peptide, a marker of cardiovascular risk. This indirect measurement involved incubation with enzyme labelled antibody, attachment of the unbound antibody at a position upstream of the SPR sensor, production of thiocholine by interaction of enzyme and acetylthiocholine in solution, and accumulation of the thiocholine on the gold SPR pad.

3.5 Raman spectroscopy

Light incident on a material may exhibit Raman scattering at shifted wavelengths (Raman 1928) due to energy being lost to molecular vibrations (Stokes shift) or imparted by them (anti-Stokes shift). Raman spectroscopy thus provides molecular fingerprint information similar to that provided by IR spectroscopy, and is a powerful technique for highly specific label-free detection of species. Raman spectroscopy has the advantage that it may be carried out at wavelengths where the absorption of water is weak and where optical instrumentation is straightforward, but has the disadvantage that the scattered signals are very weak. Several approaches have been adopted to obtain measurable signals in microfluidic systems, including surface-enhanced Raman scattering (SERS), resonance Raman scattering, and long-term integration for a stationary particle. In this section two important types of Raman spectroscopy applied to microfluidic devices are discussed.

3.5.1 Surface-enhanced Raman spectroscopy

Surface-enhanced Raman spectroscopy (SERS) exploits resonant excitation of surface plasmons on metallic surfaces to enhance Raman scattering by many orders of magnitude (Kneipp et al. 2002). Metals with a large and negative real part and a small imaginary part of dielectric permittivity, usually gold and silver, are required for efficient enhancement, and suitable surfaces for plasmon excitation include colloids, roughened and patterned films, and self-assembled structures. SERS is emerging as a competitor to fluorescence with the benefit that no tagging is required (although surface-enhanced resonance Raman (SERRS) may employ a tag) and Raman spectra show narrow lines characteristic of the material, allowing greater multiplexing. However, its application to microfluidic devices is complicated as, unlike fluorescence, the species under detection must be in close proximity to the metal surface for enhancement to take place. Reliable quantitative measurements are difficult to achieve as SERS enhancement is strongly dependent on the shape, size, and proximity of metallic features. For example, colloids are attractive enhancers in microfluidic systems as they may be analysed while flowing through the system and do not use a fixed surface within the flow channel which may become fouled. The highest enhancements using colloids occur in "hot-spots" where two particles are within a few nanometres of each other. Adequate control of measurement conditions such as the degree of colloid aggregation, particle sizes of the colloids, and the inhomogeneous distribution of molecules on a metal surface is challenging. Using a fixed patterned surface within the microflow channel has the advantage of providing a constant surface, with the disadvantage of its potential fouling and degradation.

Connatser et al. (2004) vapour deposited ~20 nm silver onto PDMS microfluidic channels to create partially embedded clusters. Raman spectroscopy was performed in a conventional Raman microscope with 633 nm laser illumination for detection of riboflavin and resorufin following CE separation in the channel. The Raman spectra for riboflavin and resorufin gave readily distinguishable peaks at wavenumber shifts of 1200 and 600 cm^{-1}, respectively. Novel structures such as nanowells patterned by soft lithography in PDMS allow more controlled production of "hot spots" for SERS, yielding enhancement factors of 10^7 in a PDMS/glass microflow channel, configured as shown in Fig. 19, compared to a device with a smooth PDMS surface (Liu and Lee 2005).

Collection of SERS spectra from flowing colloids can provide more reproducible results because of temporal averaging of the geometry and improved heat dissipation. Nirode et al. (2000) demonstrated direct on-column SERS in 100 μm diameter CE microcapillaries using silver colloids with nanomolar sensitivities for Rhodamine 6G. Flowing colloidal particles and analyte molecules show a tendency to adhere to microflow channel walls, contaminating subsequent measurements. Strehle et al. (2007) performed analysis on aqueous droplets contained within flowing lipophilic tetradecane and moved along the channel by external pumps, thereby avoiding contact between colloid and the channel walls. Crystal violet detections within the 60–180 nl droplets were performed in a concentration range of 10^{-5}–10^{-6} M, and quantification achieved by recording the amplitude of the 1177 cm^{-1} Raman peak.

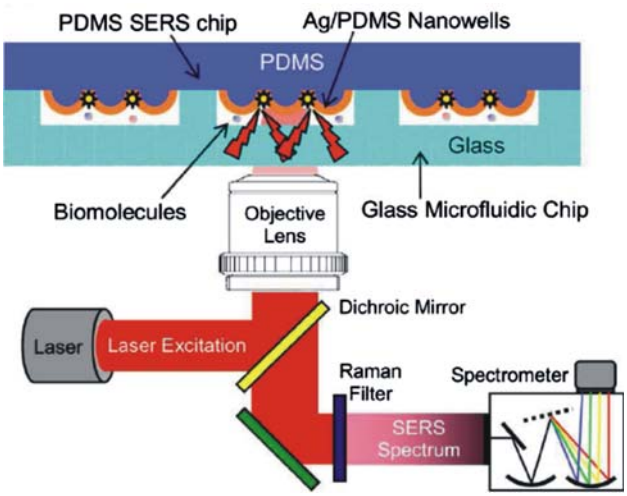

Fig. 19 Schematic diagram of integrated microfluidic chip with nanowell structures for SERS, and the Raman detection apparatus (Liu and Lee 2005). Reproduced with permission from the American Institute of Physics

Lee and co-workers realised PDMS microfluidic chips where the colloidal silver solution is mixed with the analyte using the "alligator-teeth" structure (Fig. 14b) in the microchannel, and the Raman spectrum is acquired in a downstream detection region using a conventional Raman microscope and excitation at 514.5 nm. One device was used to detect cyanide anions for pollution monitoring using a Raman peak at 2100 cm^{-1}, achieving an LoD of 1.0 ppb or below (Yea et al. 2005). Using similar devices this group also reported (1) detection of two different dye-labelled DNA nucleotides without the need for PCR or microspotting; TAMRA and Cy3 dyes were used for labelling with an LoD estimated at 10^{-11} M (Park et al. 2005), and (2) the detection of methyl parathion insecticide with an LoD of 0.1 ppm (Lee et al. 2006). Recently, again using a similar device, molecular beacons were used to hybridise with the target DNA and detected using fluorescence and SERS. In the case of the SERS measurements, silver colloids were mixed with the beacon solution and the DNA to be hybridised was added through another inlet. The Raman signal was strongly reduced if the analyte was complementary to the beacon as the change in conformation of the beacon caused the SERS-active labels to be separated from the colloid (Jung et al. 2007b).

Cooper and co-workers employed surface-enhanced resonance Raman spectroscopy (SERRS) in a microfluidic system (Keir et al. 2002; Docherty et al. 2004). The wavelength of the excitation source is selected to be at an analyte absorption, resulting in an increase in sensitivity and selectivity of the system, enabling improved discrimination of analytes from contaminants. A microfluidic device in glass was realised, in which silver colloid was formed on chip by insertion of an aqueous solution of $AgNO_3$ and of $NaBH_4$ in NaOH solution into two branches of a T-junction, producing a stream of aggregated colloids flowing down the centre of the third branch (Keir et al. 2002). The analyte was introduced at a downstream T-junction and 10 fmol of an azo dye derivative of trinitrotoluene (TNT) was detected using a conventional SERS system with 514 nm laser excitation. A similar microfluidic device was realised by the same group in PDMS, and yielded identification of up to three oligonucleotides of *E. coli* sequences labelled with different dyes (Docherty et al. 2004)

3.5.2 *Laser tweezer Raman spectroscopy*

Advances in optical trapping in microfluidic systems were described in Sect. 2. Laser tweezer Raman spectroscopy (LTRS) exploits a single-beam optical gradient trap to hold and isolate a particle while performing Raman spectroscopy upon it. Such trapping applies to larger objects such as cells, where detection of Raman scattering is less problematic, and has the advantages that the object can be held away from surroundings, to limit background interferences, can be held stationary for extended periods and then released, to allow temporal integration of spectra and improved signal to noise ratio, and can be moved in and out of the Raman probe volume, to allow background subtraction and noise reduction. The optical gradient trap has been employed for some time to study Raman spectra of levitated objects (Thurn and Kiefer 1984). However, it is only recently that LTRS has been used in conjunction with microfluidics. Xie et al. (2005) fabricated a simple microfluidic system with two microfluidic chambers joined by a microchannel. Individual yeast cells and bacteria were trapped and identified from their Raman spectra in one chamber and then moved to separate regions in the collection chamber for subsequent processing using the tweezer.

Methods to improve the sensitivity of LTRS systems by reducing or cancelling background and environmental interferences are being continually refined and incorporated in microfluidic environments. The use of separate wavelengths for trapping and Raman scattering adds an extra dimension to LTRS systems. Creely et al. (2005) realised a macrofluidic dual-wavelength LTRS system with excitation of the Raman spectra at 785 nm, and trapping at 1,064 nm. Individual living yeast cells were trapped, a Raman spectrum obtained for between 0.2 and 180 s, moved out of the Raman excitation beam so that a background measurement could be acquired under the same experimental conditions, and then the spectrum had the background subtracted. The approach employed a single microscope system using an excitation power and trapping power both <10 mW, allowing live cells to be observed for over 2 h, and detailed information on temporal changes in the cells to be obtained. Recently Rusciano et al. (2006) have demonstrated a dual-beam microfluidic system, where the Raman probe beam is kept in a fixed position whilst the trapping beam position oscillates so that the trapped object is moved through the Raman probe volume twice in each period of oscillation, thereby modulating the Raman signal by a frequency $2f$. This can then be demodulated with low noise using a lock-in amplifier, removing any stray light or unmodulated background fluorescence. The resultant signal includes a spurious component also modulated by $2f$ due to the photon scattering of the solvent volume. However, this second component is easily distinguished as it is shifted by $\pi/2$ radians with respect to the desired signal.

Dual-wavelength systems have also been realised, employing two separate microscopes, allowing greater independence in optimisation of trapping and Raman detection, and applied to red blood cells, yeast cells and resonance Raman spectroscopy of red blood cells (Geßner

et al. 2004; Ramser et al. 2004). Ramser et al (2005) have developed their approach for application to a microfluidic chip for resonance Raman spectroscopy of red blood cells (Fig. 2), allowing the oxygenation cycle of an individual erythrocyte to be studied.

In the case of detection of small numbers of biomolecules, laser tweezer Raman spectroscopy may be combined with SERS to enhance Raman signals by trapping micron-sized metal colloid clusters or metal-coated glass spheres (Xie and Li 2002; Geßner et al. 2004), and taking the Raman spectra of molecules absorbed on them.

3.6 Thermal Lens Detection

Light incident upon a liquid sample may be absorbed by the sample, which then undergoes non-radiative relaxation and heats the surrounding volume. This heat changes the refractive index of the medium, usually lowering it. If a laser excitation beam is focussed on a small volume, the refractive index change is increased and a thermal lens (TL) is created by the thermal gradient. A laser probe beam can then be used to detect these changes. A thermal lens microscope (TLM) exploits this phenomenon by focussing a coaxial excitation beam and probe beam on the fluid through an objective lens, and detecting the power in the probe beam passing through a pinhole after filtering out the excitation wavelength, as shown for nanoparticle detection in Fig. 20. A modulated excitation laser and synchronous detection is used to reduce noise and improve detection limit. Sensitivity to absorption is extremely high, as is required in microfluidic systems with small volumes, but TL is generally not able to distinguish between absorbing species, although thermal lens spectroscopy yields some compositional information. Kitamori et al. (2004), writing on the principles of TLM and its application to imaging and microfluidics, observe that the chemical specificity obtainable through separation of analyte species in microfluidics is complemented by the great sensitivity of thermal lens detection. Further miniaturisation of the TLM is required for practical use in microfluidic systems as the optics used tends to be quite bulky.

Kitamori and co-workers have made a large contribution to the development of continuous-flow chemical processing incorporating TLM in microfluidic devices, and demonstrated its potential applications, with 0.1 nM detection limits in 7 fl detection volumes, for example (Tokeshi et al. 2001). A three-dimensional microchannel network on chip with pressure-driven flow that produced multi-phase laminar flows was able to perform 20 micro operations such as mixing and liquid–liquid extraction. The device was used to extract and analyse Fe(II) and Co(II) ions using changes in absorption spectrum (Kikutani et al. 2004). A simpler device which also makes use of multi-phased flows demonstrated an LoD of 7×10^{-8} M for carbaryl pesticide, two orders of magnitude lower than conventional spectrophotometric methods for (Smirnova et al. 2006). These systems employed single wavelength excitation at 532 nm and detection at 633 nm. A tunable thermal lens spectrometer system using a Xe lamp and monochromator as excitation source (Tamaki et al. 2005) enabled determination of the thermal lens spectrum of non-scattering and turbid solutions, demonstrating a clear advantage over absorption detection by measuring the spectrum largely regardless of the strong light scattering background. The thermal gradient required for thermal lensing was obtained by exploiting rapid thermal conduction between the glass substrate and the liquid, rather than by tight focussing of the excitation beam. Application to cultured cells was demonstrated (Goto et al. 2005) by monitoring nitric oxide release from macrophage-like cells stimulated by lipopolysaccharide using a colorimetric reaction in a microfluidic device with localized temperature control. A successful assay was achieved within 4 h using 3,000 cells compared to 24 h and 10^5–10^6 cells for conventional batch methods. UV excitation TLM at 266 nm was employed for detection of adenine aqueous solutions without labelling in a fused-silica microchip. The sensitivity obtained was 350 times higher than a conventional spectrophotometric method with an LoD of 1.4×10^{-8} M (Hiki et al. 2006). Detection of single and multiple 50 nm gold nanoparticles was demonstrated using TLM, as shown in Fig. 20 and their optically driven fixation to the wall of the glass microchannel using the same beam was also demonstrated, having the potential for sensitive nanoparticles detection and production of microchip SERS substrates (Mawatari et al. 2006). A glass microchip consisting of a microchamber for cell culture connected to a microchannel for TLM detection was used to monitor intercellular messengers (Sato et al. 2006). Rat hippocampus nerve cells were

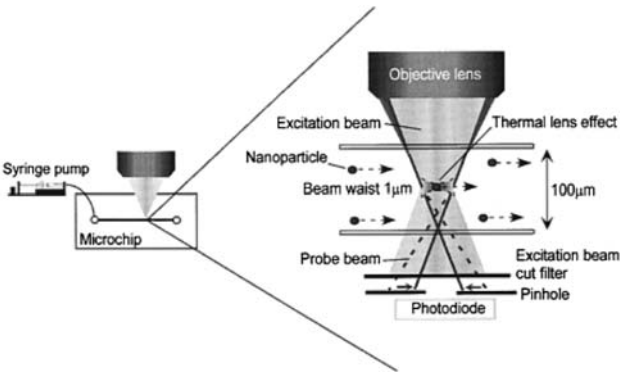

Fig. 20 Principle of detection of individual nanoparticles by thermal lens microscopy (Mawatari et al. 2006). Reproduced with permission from the Japanese Society for Analytical Chemistry

cultured in the microchamber to form a neural network, and the retrograde messenger was then detected in the microchannel. Chirality of low-volume liquid samples was measured in a microfluidic device by using TLM in which the handedness of circularly polarised excitation light was modulated (Yamauchi et al. 2006a). Left- and right-circularly polarized light may be absorbed differentially in a chiral medium, and this is detected as a modulation of the detected TLM signal. Miniaturised thermal lens systems have been realised utilizing, for example, optical fibres, fibre wavelength multiplexer for the two diode laser sources (658 nm excitation and 785 nm probe) and SELFOC microlenses. LoDs of 3.7×10^{-8} M for sunset yellow and 7.7×10^{-9} M for nickel (II) phthalocyanine-tetrasulfonic acid, tetrasodium salt (NiP) were achieved, showing a rather small reduction in performance compared with the conventional bulk-optical detection system (Tokeshi et al. 2005). Employing both TLM detection and fluorescence in a microfluidic device with similar miniaturised optics yielded an LoD 6.3 nM for (NiP) and 3 nM for Cy5 (Yamauchi et al. 2006b).

Kakuta et al. (2006) realised a semi-automated heterogeneous immunoassay system for brain natriuretic peptide (BNP), using TLM to detect BNP within a concentration range of 0.1–100 pg ml^{-1} through reaction resulting in a blue-coloured product. Kitagawa et al. (2006) used CE separation in fused silica capillaries connected to a microchannel on a chip. The system achieved an LoD of 3.6×10^{-7} M for the azo dye, Sudan Red, more than two orders of magnitude lower than that of conventional absorbance detection. Micellar electrokinetic chromatography with sample concentration by "sweeping" (Quirino and Terabe 1998) reduced the LoD to 1.2×10^{-12} M. Mawatari et al. (2005) used the sensitivity of the TLM signal to focusing position to optimise precise focusing in a portable TL apparatus, in a manner similar to the optical disk drive, using a micro-optical pick-up unit rather than a microscope. Adjustments of the depth were made by determination of the astigmatism of the reflected excitation beam, and the width by monitoring transmitted scattered light of the probe beam. An LoD of 30 nM was achieved for xylene cyanol solution, with a sensitivity between 20 and 100 times higher than that obtained by spectrophotometry. This laboratory then presented a similar miniaturised TLM system, but with reflective rather than transmissive optics, shown in Fig. 21, reducing alignment complexity, and only requiring optical access from one side of the microfluidic chip. This was achieved by forming an aluminium mirror on the reverse of the microchip. The reflected probe beam was detected with 40 times higher sensitivity when compared to a spectrophotometer, with an LoD of 60 nM for xylene cyanol solution (Mawatari and Shimoide 2006).

Ghaleb and Georges have reviewed and analysed the use of crossed-beam systems, in which the excitation beam and probe beam are perpendicular to each other, in comparison with the collinear approach normally used in TLM. In the former case, the heated sample acts as a cylindrical lens for the probe beam, and excitation light exhibits less interference with detection (Ghaleb and Georges 2004). They subsequently performed a detailed optimisation of crossed-beam systems for chopping frequency, sample size and flow rate in fused silica capillaries (Ghaleb and Georges 2005).

4 Conclusion

The miniaturised and automated laboratory, micro-total-analysis system, or LoC, presents great benefits in terms of reagent and sample consumption, speed, precision, and automation of analysis, and thus cost and ease of use, resulting in growing adoption of microfluidic approaches for practical measurements, and the potential for their widespread use in society. In this review we have discussed a representative cross-section of recent applications of optical techniques in microfluidic systems for chemical and biological analysis, with an emphasis on further miniaturisation of the optical functions.

Optical techniques are the established front-runners for high sensitivity detection in microfluidic systems. While optical telecommunications benefited from needing large numbers of devices providing a few very well defined functions, optical sensing must satisfy many very diverse applications so that the optical phenomenon to be probed and the required sensitivity, specificity, speed and cost may require a different technological solution for each

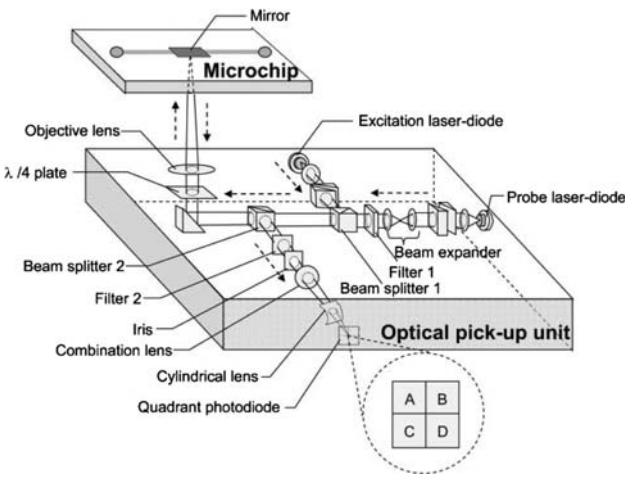

Fig. 21 Illustration of the optical arrangement of a reflective thermal lens detection device (Mawatari and Shimoide 2006). Reproduced with permission from the Royal Society of Chemistry

application (Culshaw 2004). The challenge is greater in microfluidic systems where the sample volumes and optical path-lengths are small, though this also provides advantages for single molecule or single cell analysis. Most present systems rely upon bulk-optical systems external to the fluidic chip, such as confocal microscopes, which render portable miniaturised systems difficult to realise, although this approach does have the advantage of easy reconfigurability of the optical system.

Scattering has been used to yield size and shape information on cells in flow cytometry and it is expected that further advances in interrogation of scattering distributions, perhaps combined with fluorimetry, will generate powerful new automated cell recognition and sorting systems. Detection through optical absorption is common in macrofluidic chemical analysis, often not requiring labelling; however, the short path length leads to poor detectability and a variety of approaches are being adopted to enhance absorption through using a variety of "multipass" systems and sample concentration steps. Thermal lensing is advancing fast as an extremely sensitive method of performing absorption-dependent assays not requiring long path lengths. Fluorescent detection, while usually requiring labelling, is so sensitive and has achieved such wide acceptance that it is by far the most dominant technique. The trends here are in moving to more stable tags such as quantum dots, and longer wavelength semiconductor sources for compactness, low cost and reduced background fluorescence. Improvements are also being made in geometrical configuration by incorporating multiple parallel channels, optimising fluorescence collection angle and realising compact multiwavelength chip interrogation units. Refractive index measurement is being exploited in Fabry–Perot etalon cavities for cell analysis and in evanescent approaches such as integrating dielectric waveguides or metal films supporting surface plasma waves within microchannels. These techniques do not require the use of labels and therefore need careful referencing or integration in separation systems to reduce the potential for non-specific interferences. Nonetheless the ease of mass-production of the evanescent devices using conventional microelectronics processing renders them particularly attractive for fully integrated systems. Raman spectroscopy is gaining ground in direct label-free detection and identification of species. Normally, surface enhanced Raman spectroscopy must be used to obtain sufficient signal, and this either uses nanostructured metal films on the walls of the fluidic channels, which can degrade or become blocked, or metallic nanoparticles added to the fluid to be analysed, which then flow out of the detection region with the sample after analysis. Laser-tweezer Raman spectroscopy may be used to trap and analyse larger objects such as cells without enhancement, or for species attached to enhancing beads, with the advantages that signal integration times can be long and an object can be held away from any interfering surface.

Optical trapping, manipulation and sorting, which extend the well-known optical tweezer technique, are growing in appeal, often as complements to hydrodynamic or electrokinetic approaches. Optical sorting of particles such as cells has been carried out in several different implementations by using forces dependent on the optical characteristics of the particles to modify their velocity in a flowing liquid in a novel form of chromatography. Alternatively, arrays of optical traps have been used to capture particles and release them at will; concurrent optical detection may activate the release in miniaturised versions of fluorescence-activated cell-sorters, for example. In addition to long-term trapping of cells or beads for low-noise Raman detection, optical traps have been used for other measurements on individual cells, including cell rigidity. Rather than tightly focussed single-beam traps, opposing dual-beam traps show advantages for these applications as they are more suited to large objects and, using lower intensities, are less likely to cause cell damage. Not requiring lenses, these traps are particularly simple to implement monolithically with photolithographically positioned integrated lasers or waveguides. For two-dimensional sorting in a fluidic plane, the optical potential landscape produced by interference or other patterning of a two-dimensional array of optical traps provides a particularly elegant and flexible means of separation. Evanescent techniques, where a prism or waveguide is used to generate propulsion and trapping optical forces close to a surface, have been employed for sorting, guiding and separation at a surface. This approach has the advantage that the optical path does not pass through the bulk of the sample and that the intensity distribution at the surface may be very precisely controlled. However, the optical fields only reach a few hundred nanometres into the sample, so objects to be manipulated must be very close to the surface. A wide variety of optically driven micropumps have been realised, having fewer constraints on liquid medium than electrokinetic pumps, and flexible external control of the impellors without direct electrical connection to the microfluidic chip. In some cases the micropumps are completely optically configured within the channel by collecting and controlling the motion of beads, yielding great flexibility in configuration.

This review set out to study progress towards the miniaturisation of optical functions in the LoC, where significant advances are being made in both miniaturisation of the instrumentation and on the chips themselves. The vast majority of optical functions are still carried out with bulky external optics, but it is envisaged that with closer collaboration between the optics, biosensor and microsystems communities, low-cost mass-produced integrated

systems will emerge. In the sort term, further integration of optical functions will render the LoC more costly and less flexible, but the example of the microelectronics industry shows that mass-production will ultimately bring these costs down and allow widespread use of optically integrated microsystems, if further standardisation of protocols and commonality of technological platforms can be achieved.

Acknowledgments The authors are grateful to Dr Olav Gaute Hellesø, University of Tromsø, Norway, for useful comments on the manuscript.

References

Applegate RW, Squier J, Vestad T, Oakey J, Marr DWM (2004) Optical trapping, manipulation, and sorting of cells and colloids in microfluidic systems with diode laser bars. Opt Express 12:4390–4398

Applegate RW, Squier J, Vestad T, Oakey J, Marr DWM, Bado P, Dugan MA, Said AA (2006) Microfluidic sorting system based on optical waveguide integration and diode laser bar trapping. Lab Chip 6:422–426

Ashkin A (1970) Acceleration and trapping of particles by radiation pressure. Phys Rev Lett 24:156–159

Ashkin A, Dziedzic JM, Bjorkholm JE, Chu S (1986) Observation of a single-beam gradient force optical trap for dielectric particles. Opt Lett 11:288–290

Bernini R, De Nuccio E, Brescia F, Minardo A, Zeni L, Sarro PM, Palumbo R, Scarfi MR (2006) Development and characterization of an integrated silicon micro flow cytometer. Anal Bioanal Chem 386:1267–1272

Blanco FJ, Agirregabiria M, Berganzo J, Mayora K, Elizalde J, Calle A, Dominguez C, Lechuga LM (2006) Microfluidic-optical integrated CMOS compatible devices for label-free biochemical sensing. J Micromech Microeng 16:1006–1016

Buican TN, Smyth MJ, Crissman HA, Salzman GC, Stewart CC, Martin JC (1987) Automated single-cell manipulation and sorting by light trapping. Appl Opt 26:5311–5316

Choi CJ, Cunningham BT (2006) Single-step fabrication and characterization of photonic crystal biosensors with polymer microfluidic channels. Lab Chip 6:1373–1380

Connatser RM, Riddle LA, Sepaniak MJ (2004) Metal-polymer nanocomposites for integrated microfluidic separations and surface enhanced Raman spectroscopic detection. J Sep Sci 27:1545–1550

Constable A, Kim J, Mervis J, Zarinetchi F, Prentiss M (1993) Demonstration of a fibre-optical light-force trap. Opt. Lett. 18:1867–1869

Costin CD, Olund RK, Staggemeier BA, Torgerson AK, Synovec RE (2003) Diffusion coefficient measurement in a microfluidic analyzer using dual-beam microscale-refractive index gradient detection application to on-chip molecular size determination. J Chromatogr A 1013:77–91

Craighead H (2006) Future lab-on-a-chip technologies for interrogating individual molecules. Nature 442:387–393

Cran-McGreehin SJ, Dholakia K, Krauss TF (2006a) Monolithic integration of microfluidic channels and semiconductor lasers. Opt Express 14:7723–7729

Cran-McGreehin SJ, Krauss TF, Dholakia K (2006b) Integrated monolithic optical manipulation. Lab Chip 6:1122–1124

Creely CM, Singh GP, Petrov D (2005) Dual wavelength optical tweezers for confocal Raman spectroscopy. Opt Commun 245:465–470

Culshaw B (2004) Optical fiber sensor technologies: opportunities and—perhaps—pitfalls. J Lightwave Technol 22:39–50

Datta A, Eom I-Y, Dhar A, Kuban P, Manor R, Ahmad I, Gangopadhyay S, Dallas T, Holtz M, Temkin H, Dasgupta PK (2003) Microfabrication and characterisation of Teflon AF-coated liquid core waveguide channels in silicon. IEEE Sensors J 3:788–795

deMello A (2006) Control and detection of chemical reactions in microfluidic systems. Nature 442:394–402

Destandau E, Lefevre J-P, Eddine ACF, Desportes S, Jullien MC, Hierle R, Leray I, Valeur B, Delaire JA (2007) A novel microfluidic flow-injection analysis device with fluorescence detection for cation sensing. Application to potassium. Anal Bioanal Chem. 387:2627–2632

Dholakia K, Reece P (2006) Optical micromanipulation takes hold. Nanotoday 1:18–27

Dishinger JF, Kennedy RT (2007) Serial immunoassay in parallel on a microfluidic chip for monitoring hormone secretion from living cells. Anal Chem 79:947–954

Dittrich PS, Manz A (2005) Single-molecule fluorescence detection in microfluidic channels-the Holy Grail in μTAS? Anal Bioanal Chem 382:1771–1782

Dittrich PS, Tachikawa K, Manz A (2006) Micro total analysis systems. Latest advancements and trends. Anal Chem 78:3887–3907

Docherty FT, Monaghan PB, Keir R, Graham D, Smith WE, Cooper JM (2004) The first SERRS multiplexing from labelled oligonucleotides in a microfluidics lab-on-a-chip. Chem Commun (1):118–119

Duggan MP, McCreedy T, Aylott JW (2003) A non-invasive analysis method for on-chip spectrophotometric detection using liquid-core waveguiding within a 3D architecture. Analyst 128:1336–1340

Duveneck GL, Abel AP, Bopp MA, Kresbach GM, Ehrat M (2002) Planar waveguides for ultra-high sensitivity of the analysis of nucleic acids. Anal Chim Act 469:49–61

Edgar JS, Pabbati CP, Lorenz RM, He M, Fiorini GS, Chiu DT (2006) Capillary electrophoresis separation in the presence of an immiscible boundary for droplet analysis. Anal Chem 78:6948–6954

El-Ali J, Sorger PK, Jensen KF (2006) Cells on chips. Nature 442:403–411

Erickson D, Li D (2004) Integrated microfluidic devices. Anal Chim Act 507:11–26

Flynn RA, Birkbeck AL, Gross M, Ozkan M, Shao B, Wang MM, Esener SC (2002) Parallel transport of biological cells using individually addressable VCSEL arrays as optical tweezers. Sens Actuators B 87:239–243

Fu AY, Spence C, Scherer A, Arnold FH, Quake SR (1999) Nat Biotech 17:1109–1111

Fu J-L, Fang Q, Zhang T, Jin X-H, Fang Z-L (2006) Laser-induced fluorescence detection system for microfluidic chips based on an orthogonal optical arrangement. Anal Chem 78:3827–3834

Furuki M, Kameoka J, Craighead HG, Isaacson MS (2001) Surface plasmon resonance sensors utilizing microfabricated channels. Sens Actuators 79:63–69

Garcés-Chávez V, Dholakia K, Spalding GC (2005) Extended-area optically induced organization of microparticles on a surface. Appl Phys Lett 86:031106

Gaugiran S, Gétin S, Fedeli JM, Colas G, Fuchs A, Chatelin F, Dérouard J (2005) Optical manipulation of microparticles and cells on silicon nitride waveguides. Opt Express 13:6956–6963

Geßner R, Winter C, Rösch, Schmitt M, Petry R, Kiefer W, Lamkers M, Popp J (2004) Identification of biotic and abiotic particles by using a combination of optical tweezers and in situ Raman spectroscopy. Chem Phys Chem 5:1159–1170

Ghaleb KA, Georges J (2004) Photothermal spectrometry for detection in miniaturized systems: relevant features, strategies and recent applications. Spectrochim Acta Part A 60:2793–2801

Ghaleb KA, Georges J (2005) Signal optimisation in cw-laser crossed-beam photothermal spectrometry: influence of the chopping frequency, sample size and flow rate. Spectrochim Acta Part A 61:2849–2855

Gong M, Wehmeyer KR, Limbach PA, Arias F, Heineman WR (2006) On-line sample preconcentration using field-amplified stacking injection in microchip capillary electrophoresis. Anal Chem 78:3730–3737

Goto M, Sato K, Murakami A, Tokeshi M, Kitamori T (2005) Development of a microchip-based bioassay system using cultured cells. Anal Chem 77:2125–2131

Götz S, Karst U (2007a) Recent developments in optical detection methods for microchip separations. Anal Bioanal Chem 387:183–192

Götz S, Karst U (2007b) Wavelength-resolved fluorescence detector for microchip capillary electrophoresis separations. Sens Actuators B 123:622–627

Götz S, Revermann T, Karst U (2007c) Quantitative on-chip determination of taurine in energy and sports drinks. Lab Chip 7:93–97

Grujic K, Hellesø OG, Hole JP, Wilkinson JS (2005) Sorting of polystyrene microspheres using a Y-branched optical waveguide. Opt Express 13:1–7

Grumann M, Stiegert J, Riegger L, Moser I, Enderle B, Riebeseel K, Urban G, Zengerle R, Ducrée (2006) Sensitivity enhancement for colorimetric glucose assays on whole blood by on-chip beam-guidance. Biomed Microdevices 8:209–214

Guck J, Schinkinger S, Lincoln B, Wottawah F, Ebert S, Romeyke M, Lenz D, Erickson HM, Ananthakrishnan, Mitchell D, Käs, Ulvick S, Bilby C (2005) Optical deformability as an inherent cell marker for testing malignant transformation and metastatic competence. Biophys J 88:3689–3698

Haes AJ, Terray A, Collins GE (2006) Bead-assisted displacement immunoassay for staphylococcal enterotoxin B on a microchip. Anal Chem 78:8412–8420

Hart SJ, Terray A, Leski TA, Arnold J, Stroud R (2006) Discovery of a significant optical chromatographic difference between spores of *Bacillus anthracis* and its close relative, *Bacillus thuringiensis*. Anal Chem 78:3221–3225

Hart SJ, Terray A, Arnold J, Leski TA (2007) Sample concentration using optical chromatography. Opt Express 15:2724–2731

Heideman RG, Lambeck PV (1999) Remote opto-chemical sensing with extreme sensitivity: design, fabrication and performance of a pigtailed integrated optical phase-modulated Mach–Zehnder interferometer system. Sensors Actuat B 61:100–127

Hellmich W, Greif D, Pelargus C, Anselmetti D, Ros A (2006) Improved native UV laser induced fluorescence detection for single cell analysis in poly(dimethylsiloxane) microfluidic devices. J Chromatogr A 1130:195–200

Hiki S, Mawatari K, Hibara A, Tokeshi M, Kitamori T (2006) UV excitation thermal lens microscope for sensitive and nonlabeled detection of nonfluorescent molecules. Anal Chem 78:2859–2863

Hofmann O, Wang X, Cornwell A, Beecher S, Raja A, Bradley DDC, deMello AJ, deMello JC (2006) Monolithically integrated dye-doped PDMS long-pass filters for disposable on-chip fluorescence detection. Lab Chip 6:981–987

Hole JP, Wilkinson JS, Grujic K, Hellesø OG (2005) Velocity distribution of gold nanoparticles trapped on an optical waveguide. Opt Express 13:3896–3901

Hollars CW, Puls J, Olgica B, Olsan B, Talley CE, Lane SM, Huser T (2006) Bio-assay based on single molecule fluorescence detection in microfluidic channels. Anal Bioanal Chem 385:1384–1388

Holmes D, Morgan H, Green NG (2006) High throughput particle analysis: combining dielectrophoresis article focussing with confocal optical detection. Biosens Bioelectron 21:1621–1630

Hu J, Tarasov V, Agarwal A, Kimerling L, Carlie N, Petit L, Richardson K (2007) Fabrication and testing of planar chalcogenide waveguide integrated microfluidic sensor. Opt Express 15:2307–2314

Huang F-C, Liao C-S, Lee G-B (2006a) An integrated microfluidic chip for DNA/RNA amplification, electrophoresis separation and on-line optical detection. Electrophoresis 27:3297–3305

Huang S-C, Lee G-B, Chien F-C, Chen S-J, Chen W-J, Yang M-C (2006b) A microfluidic system with integrated molecular imprinting polymer films for surface plasmon resonance detection. J Micromech Microeng 16:1251–1257

Huang B, Wu H, Bhaya D, Grossman A, Granier S, Kobilka BK, Zare RN (2007) Counting low-copy number proteins in a single cell. Science 315:81–84

Imasaka T (1998) Optical chromatography. A new tool for separation of particles. Analusis 26:M53–M55

Inatomi K-I, Izuo S-I, Lee S-S (2006) Application of a microfluidic device for counting of bacteria. Lett Appl Microbiol 43:296–300

Irawan R, Tay CM, Tjin SC, Fu CY (2006) Compact fluorescence detection using in-fiber microchannels-its potential for lab-on-a-chip applications. Lab Chip 6:1095–1098

Jess PRT, Garcés-Chávez V, Smith D, Mazilu M, Paterson L, Riches A, Herrington CS, Sibbett W, Dholakia K (2006) Dual beam fibre trap for Raman microspectroscopy of single cells. Opt Express 14:5779–5791

Jiang L, Pau S (2007) Integrated waveguide with a microfluidic channel in spiral geometry for spectroscopic applications. Appl Phys Lett 90:111108

Jung B, Zhu Y, Santiago JG (2007a) Detection of 100 aM fluorophores using a high-sensitivity on-chip CE system and transient isotachophoresis. Anal Chem 79:345–349

Jung J, Chen L, Lee S, Kim S, Seong GH, Choo J, Lee EK, Oh C-H, Lee S (2007b) Fast and sensitive DNA analysis using changes in the FRET signals of molecular beacons in a PDMS microfluidic channel. Anal Bioanal Chem 387:2609–2615

Kakuta M, Takahashi H, Kazuno S, Murayama K, Ueno T, Tokeshi M (2006) Development of the microchip-based repeatable immunoassay system for clinical diagnosis. Meas Sci Technol 17:3189–3194

Kamei T, Wada T (2006) Contact-lens type of micromachined hydrogenated amorphous Si fluorescence detector coupled with microfluidic electrophoresis devices. Appl Phys Lett 89:114101

Kamei T, Toriello NM, Lagally ET, Blazej RG, Scherer JR, Street RA, Mathies RA (2005) Microfluidic genetic analysis with an integrated a-Si:H detector. Biomed Microdevices 7:147–152

Kawata S, Sugiura T (1992) Movement of micrometer-sized particles in the evanescent field of a laser beam. Opt Lett 17:772–774

Kawata S, Tani T (1996) Optically-driven Mie particles in an evanescent field along a channeled waveguide. Opt Lett 21:1768–1770

Keir R, Igata E, Arundell M, Smith WE, Graham D, McHugh C, Cooper JM (2002) SERRS. In situ substrate formation and improved detection using microfluidics. Anal Chem 74:1503–1508

Kelemen L, Valkai S, Ormos P (2006) Integrated optical motor. Appl Opt 45:2777–2780

Khademhosseini A, Yeh J, Eng G, Karp J, Kaji H, Borenstein J, Farokhzad OC, Langer R (2005) Cell docking inside microwells within reversibly sealed microfluidic channels for fabricating multiphenotype cell arrays. Lab Chip 5:1380–1386

Kim Y-H, Shin K-S, Kang J-Y, Yang E-G, Paek K-K, Seo D-S, Ju B-K (2006) Poly(dimethylsiloxane)-based packaging technique for microchip fluorescence detection system applications. J MEMS 15:1152–1158

Kim S, Chen L, Lee S, Seong GH, Choo J, Lee EK, Oh C-H, Lee S (2007) Rapid DNA hybridisation analysis using a PDMS Microfluidic sensor and a molecular beacon. Anal Sci 23:401–405

Kikutani Y, Hisamoto H, Tokeshi M, Kitamori T (2004) Micro wet analysis system using multi-phase laminar flows in three-dimensional microchannel network. Lab Chip 4:328–332

Kitamori T, Tokeshi M, Hibara A, Sato K (2004) Thermal lens microscopy and microchip chemistry. Anal Chem 76:52A–60A

Kitagawa F, Tsuneka T, Akimoto Y, Sueyoshi K, Uchiyama K, Hattori A, Otsuka K (2006) Toward million-fold sensitivity enhancement by sweeping in capillary electrophoresis combined with thermal lens microscopic detection using an interface chip. J Chromatogr A 1106:36–42

Kneipp K, Kneipp H, Itzkan I, Dasari RR, Feld MS (2002) Surface-enhanced Raman scattering and biophysics. J Phys Condens Matter 14:R597–R624

Korda PT, Spalding GC, Grier DG (2002) Evolution of a colloidal critical state in an optical pinning potential landscape. Phys Rev B 66:024504

Kurita R, Yokota Y, Sato Y, Mizutani F, Niwa O (2006) On-chip enzyme immunoassay of a cardiac marker using a microfluidic device combined with a portable surface plasmon resonance system. Anal Chem 78:5525–5531

Ladavac K, Grier DG (2004) Microoptomechanical pumps assembled and driven by holographic optical vortex arrays. Opt Express 12:1144–1149

Lambeck PV (2006) Integrated optical sensors for the optical domain. Meas Sci Technol 17:R93–R116

Leach J, Mushfique H, di Leonardo R, Padgett M, Cooper J (2006) An optically driven pump for microfluidics. Lab Chip 6:735–739

Lechuga LM (2007) New frontiers in optical biosensing. In: Proceedings of 13th European conference on integrated optics (ECIO 2007) Copenhagen, Paper FPT2

Lee D, Lee S, Seong GH, Choo J, Lee EK, Gweon D-G, Lee S (2006) Quantitative analysis of methyl parathion pesticides in a polydimethylsiloxane microfluidic channel using confocal surface-enhanced Raman Spectroscopy. Appl Spectrosc 60:373–377

Lei KF, Law WC, Suen Y-K, Li WJ, Yam Y, Ho HP, Kong S-K (2007) A vortex pump-based optically-transparent microfluidic platform for biotech and medical applications. J Eng Med 221:129–141

Leung S-A, Edel JB, Wootton RCR, deMello AJ (2004) Continuous real-time bubble monitoring in microchannels using refractive index detection. Meas Sci Technol 15:290–296

Li H-F, Cai ZW, Lin J-M (2006) Separation of catecholamines by microchip electrophoresis with a simple integrated laser-induced fluorescence detector. Anal Chim Acta 565:183–189

Liang Z, Chiem N, Ocvirk G, Tang T, Fluri K, Harrison DJ (1996) Microfabrication of a planar absorbance and fluorescence cell for integrated capillary electrophoresis devices. Anal Chem 68:1040–1046

Liu GL, Lee LP (2005) Nanowell surface enhanced Raman scattering arrays fabricated in soft-lithography for label-free biomolecular detections in integrated microfluidics. Appl Phys Lett 87:074101

Liu D, Zhou X, Zhong R, Ye N, Chang G, Xiong W, Mei X, Lin B (2006) Analysis of multiplex PCR fragments with PMMA microchip. Talanta 68:616–622

Liu P, Seo TS, Beyor N, Shin K-J, Scherer JR, Mathies RA (2007) Integrated portable polymerase chain reaction-capillary electrophoresis microsystem for rapid forensic short tandem repeat typing. Anal Chem 79:1881–1889

Llobera A, Wilke R, Büttgenbach S (2004) Poly(dimethylsiloxane) hollow Abbe prism with microlenses for detection based on absorption and refractive index shift. Lab Chip 4:24–27

Llobera A, Wilke R, Büttgenbach S (2005) Optimization of poly(dimethylsiloxane) hollow prisms for optical sensing. Lab Chip 5:506–511

Ma B, Zhou X, Wang G, Huang H, Dai Z, Qin J, Lin B (2006) Integrated isotachophoretic preconcentration with zone electrophoresis separation on a quartz microchip for UV detection of flavonoids. Electrophoresis 27:4904–4909

MacDonald MP, Spalding GC, Dholakia K (2003) Microfluidic sorting in an optical lattice. Nature 426:421–424

MacDonald MP, Neale S, Paterson L, Richies A, Dholakia K, Spalding GC (2004) Cell cytometry with a light touch: sorting microscopic matter with an optical lattice. J Biol Regul Homeost Agents 18:200–205

Malmqvist M (1993) Biospecific interaction analysis using biosensor technology. Nature 361:186–187

Manz A, Graber N, Widmer HM (1990) Miniaturized total chemical-analysis systems—a novel concept for chemical sensing. Sens Actuators B 1:244–248

Maruo S, Inoue H (2006) Optically driven micropump produced by three-dimensional two-photon microfabrication. Appl Phys Lett 89:144101

Mawatari K, Shimoide (2006) Reflective thermal lens detection device. Lab Chip 6:127–130

Mawatari K, Naganuma Y, Shimoide K (2005) Portable thermal lens spectrometer with focusing system. Anal Chem 77:687–692

Mawatari K, Tokeshi M, Kitamori T (2006) Quantitative detection and fixation of single and multiple gold nanoparticles on a microfluidic chip by thermal lens microscope. Anal Sci 22:781–784

Mazurczyk R, Vieillard J, Bouchard A, Hannes B, Krawczyk S (2006) A novel concept of the integrated fluorescence detection system and its application in a lab-on-a-chip microdevice. Sens Actuators B 118:11–19

McClain MA, Culbertson CT, Jacobson SC, Ramsey JM (2001) Flow cytometry of *Escherichia coli* on microfluidic devices. Anal Chem 73:5334–5338

Mellor CD, Bain CD (2006) Array formation in evanescent waves. Chem Phys Chem 7:329–332

Miller SE (1969) Integrated optics: an introduction. Bell Syst Tech J 48:2059–2069

Milne G, Rhodes D, MacDonald M, Dholakia K (2007) Fractionation of polydisperse colloid with acousto-optically generated potential energy landscapes. Opt Lett 32:1144–1146

Mitchell GL (1977) Absorption spectroscopy in scattering samples using integrated-optics. IEEE J Quantum Electron 13:173–176

Mitra B, Wilson CG, Que L, Selvaganapathy P, Gianchandani Y (2006) Microfluidic discharge-based optical sources for detection of biochemicals. Lab Chip 6:60–65

Mogensen KB, Petersen NJ, Hübner J, Kutter JP (2001) Monolithic integration of optical waveguides for absorbance detection in microfabricated electrophoresis devices. Electrophoresis 22:3930–3938

Mogensen KB, El-Ali J, Wolff A, Kutter JP (2003) Integration of polymer waveguides for optical detection in microfabricated chemical analysis systems. Appl Opt 42:4072–4079

Mogensen KB, Eriksson F, Gustafsson O, Nikolajsen RPH, Kutter JP (2004) Pure-silica optical waveguides, fiber couplers, and high-aspect ratio submicrometer channels for electrokinetic separation devices. Electrophoresis 25:3788–3795

Morgan H, Holmes D, Green NG (2006) High speed simultaneous single particle impedance and fluorescence analysis on a chip. Curr Appl Phys 6:367–370

Moring SE, Reel RT, van Soest REJ (1993) Optical improvements of a Z-shaped cell for high-sensitivity UV absorbance detection in capillary electrophoresis. Anal Chem 65:3454–3459

Mortensen NA, Xiao S (2007) Slow-light enhancement of Beer-Lambert-Bouguer absorption. Appl Phys Lett 90:141108

Neale SL, MacDonald MP, Dholakia K, Krauss TF (2005) All-optical control of microfluidic components using form birefringence. Nat Mater 4:530–533

Neuman KC, Chadd EH, Liou GF, Bergman K, Block SM (1999) Characterization of photodamage to *Escherichia coli* in optical traps. Biophys J 77:2856–2863

Nirode WF, Devault GL, Sepaniak MJ, Cole RO (2000) On-column surface-enhanced Raman spectroscopy detection in capillary electrophoresis using running buffers containing silver colloidal solutions. Anal Chem 72:1866–1871

Oh S-H, Lee S-H, Kenrick SA, Daugherty PS, Soh HT (2006) Microfluidic protein detection through genetically engineered bacterial cells. J Proteome Res 5:3433–3437

Ozkan M, Wang M, Ozkan C, Flynn R, Birkbeck A, Esener S (2003) Optical manipulation of objects and biological cells in microfluidic devices. Biomed Microdev 5:61–67

Pamme N, Koyama R, Manz A (2003) Counting and sizing of particles and particle agglomerates in a microfluidic device using laser light scattering: application to a particle-enhanced immunoassay. Lab Chip 3:187–192

Pamme N, Eijkel JCT, Manz A (2006) On-chip free-flow magnetophoresis: Separation and detection of mixtures of magnetic particles in continuous flow. J Magn Magn Mater 307: 237–244

Park T, Lee S, Seong GH, Choo J, Lee EK, Kim YS, Ji WH, Hwang SY, G D-G, Lee S (2005) Highly sensitive signal detection of duplex dye-labelled DNA oligonucleotides in a PDMS microfluidic chip: confocal surface-enhanced Raman spectroscopic study. Lab Chip 5:437–442

Paterson L, Papagiakoumou E, Milne G, Garcés-Chávez V, Tatarkova SA, Sibbett W, Gunn-Moore FJ, Bryant PE, Riches AC, Dholakia K (2005) Light-induced cell separation in a tailored optical landscape. Appl Phys Lett 87:123901

Phillips KS, Cheng Q (2007) Recent advances in surface plasmon resonance based techniques for bioanalysis. Anal Bioanal Chem 387:1831–1840

Pregibon DC, Toner M, Doyle PS (2007) Multifunctional encoded particles for high-throughput biomolecule analysis. Science 315:1393–1396

Prikulis J, Svedberg F, Käll M, Enger J, Ramser K, Godsör M, Hanstorp D (2004) Optical spectroscopy of single trapped metal nanoparticles in solution. Nano Lett 4:115–118

Psaltis D, Quake SR, Yang C (2006) Developing optofluidic technology through the fusion of microfluidics and optics. Nature 442:381–386

Quigley GR, Harris RD, Wilkinson JS (1999) Sensitivity enhancement of integrated optical sensors by use of thin high-index films. Appl Opt 38:6036–6039

Quirino JP, Terabe S (1998) Exceeding 5000-fold concentration of dilute analytes in micellar electrokinetic chromatography. Science 282:465–468

Raman CV (1928) A new type of secondary radiation. Nature 121:501–502

Ramser K, Logg K, Goksör M, Engar J, Käll M, Hanstorp D (2004) Resonance Raman spectroscopy of optically trapped functional erythrocytes. J Biomed Opt 9:593–600

Ramser K, Engar J, Goksör M, Hanstorp D, Logg K, Käll M (2005) A microfluidic system enabling Raman measurements of the oxygenation cycle in single optically trapped red blood cells. Lab Chip 5:431–436

Revermann T, Götz S, Karst U (2007) Quantitative analysis of thiols in consumer products on a microfluidic CE chip with fluorescence detection. Electrophoresis 28:1154–1160

Riegger L, Grumann, Nann T, Riegler J, Ehlert O, Bessler W, Mittenbuehler K, Urban G, Pastewka L, Brenner T, Zengerle R, Ducreé J (2006) Read-out concepts for multiplexed bead-based fluorescence immunoassays on centrifugal microfluidic platforms. Sens Actuator A 126:455–462

Ro KW, Lim K, Shim BC, Hahn JH (2005) Integrated light collimating system for extended optical-path-length absorbance detection in microchip-based capillary electrophoresis. Anal Chem 77:5160–5166

Rusciano G, De Luca AC, Sasso A, Pesce G (2006) Phase sensitive detection in Raman tweezers. Appl Phys Lett 89:261116

Salimi-Moosavi H, Jiang Y, Lester L, McKinnon G, Harrison DJ (2000) A multireflection cell for enhanced absorbance detection in microchip-based capillary electrophoresis devices. Electrophoresis 21:1291–1299

Sarov Y, Ivanov T, Ivanova K, Sarova V, Capek I, Rangelow IW (2006) Diffraction under total internal reflection for micro-fluidic analysis. Appl Phys A 84:191–196

Sato K, Egami A, Odake T, Tokeshi M, Aihara M, Kitamori T (2006) Monitoring of intercellular messengers released from neuron networks cultured in a microchip. J Chromatogr A 1111:228–232

Schroll RD, Wunenburger R, Casner A, Zhang WW, Delville J-P (2007) Liquid transport due to light scattering. Phys Rev Lett 98:133601

Schrum DP, Culbertson CT, Jacobson SC, Ramsey JM (1999) Microchip flow cytometry using electrokinetic focusing. Anal Chem 71:4173–4177

Sepúlveda B, Sánchez del Río J, Moreno M, Blanco FJ, Mayora K, Domínguez C, Lechuga LM (2006) Optical biosensor microsystems based on the integration of highly sensitive Mach–Zehnder interferometer devices. J Opt A Pure Appl Opt 8:S561–S566

Shao H, Kumar D, Lear KL (2006) Single-cell detection using optofluidic intracavity spectroscopy. IEEE Sensors J 6:1543–1550

Shen Z, Liu X, Long Z, Liu D, Ye N, Qin J, Dai Z, Lin B (2006) Parallel analysis of biomolecules on a microfabricated capillary array chip. Electrophoresis 27:1084–1092

Simonnet C, Groisman A (2006) High-throughput and high-resolution flow cytometry in molded microfluidic devices. Anal Chem 78:5653–5663

Smirnova A, Mawatari K, Hibara A, Proskurnin MA, Kitamori T (2006) Micro-multiphase laminar flows for the extraction and detection of carbaryl derivative. Anal Chim Acta 558:69–74

Smit M, Hill M, Baets R, Bente E, Dorren H, Karouta F, Koenraad P, Koonen T, Leitjens X, Nötzel, Oei S, de Waardt H, van der Tol J, Khoe D (2007) How complex can integrated optical circuits become? In: Proceedings of 13th European conference on integrated optics (ECIO 2007) Copenhagen, Paper ThPT2

Song WZ, Zhang XM, Liu AQ, Lim CS, Yap PH, Hosseini HMM (2006) Refractive index measurement of single living cells using on-chip Fabry–Perot cavity. Appl Phys Lett 89:203901

Soughayer JS, Krasieva T, Jacobson SC, Ramsey JM, Tromberg BJ, Allbritton NL (2000) Characterisation of cellular optoporation with distance. Anal Chem 72:1342–1347

Strehle KR, Cialla D, Rösch P, Hankel T, Köhler, Popp J (2007) A reproducible surface-enhanced Raman spectroscopy approach. online SERS measurements in a segmented microfluidic system. Anal Chem 79:1542–1547

Sun Y, Yin X-F (2006a) Novel multi-depth microfluidic chip for single cell analysis. J Chromatogr A 1117:228–233

Sun YY, Ong LS, Yuan X-C (2006b) Composite-microlens-array-enabled microfluidic sorting. Appl Phys Lett 89:141108

Svoboda K, Block SM (1994) Optical trapping of metallic Rayleigh particles. Optics Letters 19:930–932
Tamaki E, Hibara A, Tokeshi M, Kitamori T (2005) Tunable thermal lens spectrometry utilizing microchannel-assisted thermal lens spectrometry. Lab Chip 5:129–131
Terray A, Oakey J, Marr DWM (2002) Microfluidic control using colloidal devices. Science 296:1841–1844
Terray A, Arnold J, Hart SJ (2005) Enhanced optical chromatography in a PDMS microfluidic system. Opt Express 13:10406–10415
Tokeshi M, Uchida M, Hibara A, Sawada T, Kitamori T (2001) Determination of subyoctomole amounts of nonfluorescent molecules using a thermal lens microscope: subsingle-molecule determination. Anal Chem 73:2112–2116
Tokeshi M, Yamaguchi J, Hattori A, Kitamori T (2005) Thermal lens micro optical systems. Anal Chem 77:626–630
Thurn R, Kiefer W (1984) Raman-microsampling technique applying optical levitation by radiation pressure. Appl Spectrosc 38:78–83
Veldhuis GJ, Parriaux O, Hoekstra HJWM, Lambeck PV (2000) Sensitivity enhancement in evanescent optical waveguide sensors. J Lightwave Technol 18:677–682
Viskari PJ, Landers JP (2006) Unconventional detection methods for microfluidic devices. Electrophoresis 27:1797–1810
Wang Z, El-Ali J, Engelund M, Gotsaed T, Perch-Nielsen IR, Mogensen KB, Snakenborg D, Kutter JP, Wolff A (2004) Measurements of scattered light on a microchip flow cytometer with integrated polymer based optical elements. Lab Chip 4:372–377
Wang MM, Tu E, Raymond DE, Yang JM, Zhang H, Hagenb N, Dees B, Mercer EM, Forster AH, Kariv I, Marchand PJ, Butler WF (2005) Microfluidic sorting of mammalian cells by optical force switching. Nat Biotech 23:83–87
Wang Z, Hansen O, Petersen PK, Rogeberg A, Kutter JP, Bang DD, Wolff A (2006) Dielectrophoresis microsystem with integrated flow cytometers for on-line monitoring of sorting efficiency. Electrophoresis 27:5081–5092
Wheeler AR, Chah S, Whelan RJ, Zare RN (2004) Poly(dimethylsiloxane) microfluidic flow cells for surface plasmon resonance spectroscopy. Sens Actuators B 98:208–214
Witek MA, Wei S, Vaidya B, Adams AA, Zhu L, Stryjewski W, McCarley RL, Soper SA (2004) Cell transportation via electromigration in polymer-based microfluidic devices. Lab Chip 4:464–472
Xia YN, Whitesides GM (1998) Soft lithography. Ann Rev Mater Sci 28:153–184
Xiang Q, Hu G, Gao Y, Li D (2006) Miniaturized immunoassay microfluidic system with Electrokinetic control. Biosens Bioelectron 21:2006–2009
Xie C, Li Y-Q (2002) Raman spectra and optical trapping of highly refractive and non-transparent particles. Appl Phys Lett 81:951–953
Xie C, Chen D, Li Y-Q (2005) Raman sorting and identification of single living micro-organisms with optical tweezers. Opt Lett 30:1800–1802
Yamaguchi N, Ohba H, Nasu M (2006) Simple detection of small amounts of *Pseudomonas* cells in milk by using a microfluidic device. Lett Appl Microbiol 43:631–636
Yamauchi M, Mawatari K, Hibara A, Tokeshi M, Kitamori T (2006a) Circular dichroism thermal lens microscope for sensitive chiral analysis on microchip. Anal Chem 78:2646–2650
Yamauchi M, Tokeshi M, Yamaguchi J, Fukuzawa T, Hattori A, Hibara A, Kitamori T (2006b) Miniaturized thermal lens and fluorescence detection system for microchemical chips. J Chromatogr A 1106:89–93
Yan Q, Chen RS, Cheng J-K (2006) Highly sensitive fluorescence detection with Hg-lamp and photon counter in microchip capillary electrophoresis. Anal Chim Acta 555:246–249
Yang S-Y, Hsiung S-K, Hung Y-C, Chang C-M, Liao T-L, Lee G-B (2006) A cell counting/sorting system incorporated with a microfabricated flow cytometer chip. Meas Sci Technol 17:2001–2009
Yea K-H, Lee S, Kyong JB, Choo J, Lee EK, Joo S-W, Lee S (2005) Ultra-sensitive trace analysis of cyanide water pollutant in a PDMS microfluidic channel using surface-enhanced Raman spectroscopy. Analyst 130:1009–1011
Yea K-H, Lee S, Choo J, Oh C-H, Lee S (2006) Fast and sensitive analysis of DNA hybridization in a PDMS micro-fluidic channel using fluorescence resonance energy transfer. Chem Commun (14):1509–1511
Yeh H-C, Puleo CM, Lim TC, Ho Y-P, Giza PE, Huang RCC, Wang T-H (2006) A microfluidic-FCS platform for investigation on the dissociation of Sp1-DNA complex by doxorubicin. Nucleic Acids Res 34:e144–e152
Yi C, Li C-W, Ji S, Yang M (2006a) Microfluidics technology for manipulation and analysis of biological cells. Anal Chim Act 560:1–23
Yi C, Zhang Q, Li C-W, Yang J, Zhao J, Yang M (2006b) Optical and electrochemical detection techniques for cell-based microfluidic systems. Anal Bioanal Chem 384:1259–1268
Ymeti A, Kanger JS, Greve J, Besselink GAJ, Lambeck PV, Wijn RR, Heideman RG (2005) Integration of microfluidics with a four-channel integrated optical Young interferometer immunoassay. Biosens Bioelectron 20:1417–1421
Ymeti A, Greve J, Lambeck PV, Wink T, van Hövell SWFM, Beumer TAM, Wijn RR, Heideman RG, Subramaniam V, Kanger JS (2007) Fast, ultrasensitive virus detection using a Young interferometer sensor. Nano Lett 7:394–397
Yuen PK, Fontaine NH, Quesada MA, Mazumder P, Bergman R, Mozdy EJ (2005) Self-referencing a single waveguide-grating sensor in a micron-sized deep flow chamber for label-free biomolecular binding assays. Lab Chip 5:959–965
Yun K-S, Lee D, Kim H-S, Yoon E (2006) A microfluidic chip for measurement of biomolecules using microbead-based quantum dot fluorescence assay. Meas Sci Technol 17:3178–3183
Zhang H, Tu E, Hagen ND, Schnabel CA, Paliotti MJ, Hoo WS, Nguyen PM, Kohrumel JR, Butler WF, Chachisvillis, Marchand PJ (2004) Time-of-flight optophoresis analysis of live whole cells in microfluidic channels. Biomed Microdevices 6:11–21
Zhang Y, Bahns J, Jin Q, Divan R, Chen L (2006) Toward the detection of a single virus particle in serum. Anal Biochem 356:161–170
Zhu L, Lee CS, DeVoe DL (2006) Integrated microfluidic UV absorbance detector with attomol-level sensitivity for BSA. Lab Chip 6:115–120